치의과학박사 학위논문

Development of repositioning method of maxillomandibular complex under movable head position using robot with 3D position recognizing function and navigation system in orthognathic surgery

턱교정수술에서 로봇의 위치 인식 기능과 네비게이션 시스템을 이용하여 두부 움직임의 조건에서 상하악 복합체 재위치 방법의 개발

2019 년 2 월

서울대학교 대학원

치의과학과 구강악안면외과학전공

박 재 봉

Development of repositioning method of maxillomandibular complex under movable head position using robot with 3D position recognizing function and navigation system in orthognathic surgery

지도 교수 황 순 정

이 논문을 치의과학박사 학위논문으로 제출함
2019년 2월

서울대학교 대학원
치의과학과 구강악안면외과학전공
박 재 봉

박재봉의 박사학위논문을 인준함
2019년 2월

위 원 장 _____ 이 원 진 (인)

부위원장 _____ 황 순 정 (인)

위 원 _____ 김 성 민 (인)

위 원 _____ 임 원 희 (인)

위 원 _____ 허 종 기 (인)

-Abstract-

Development of repositioning method of maxillomandibular complex under movable head position using robot with 3D position recognizing function and navigation system in orthognathic surgery

Jae Bong Park, D.D.S., M.S.D.

Program in Oral and Maxillofacial Surgery, Department of Dental Science, Graduate School, Seoul National University

(Directed by Professor Soon Jung Hwang, Dr. med. Dr. med. Dent)

Background

For a long time, oral and maxillofacial surgeons conducted a study on accurate establishment of surgical treatment objectives (STOs) and moving the maxilla in accordance with STOs. Advances in CAD/CAM and 3D printing technologies have developed ways to overcome many errors. Real-time navigation systems were also designed to verify that the

maxillomandibular complex was positioned as planned during surgery. However, even with navigation equipment, repositioning the maxilla is not accurate and time consuming due to hand tremors. To overcome these limitations, studies have used a robot arm in conjunction with a navigation system.

In this study, we developed a method to reposition a maxillomandibular complex under a head movement condition using the 3D position recognizing function of the robot and a navigation system. In addition, we designed and fabricated an osteotomy guide template that can remove the predicted interference during Le Fort I osteotomy in robot-assisted and navigation-assisted orthognathic surgery.

Materials and methods

A total of 12 phantom skull models were used and divided into four groups according to STO.

I. Using the simulation program, interferences when the osteotomized maxilla is repositioned to the planned location are confirmed in advance. In order to remove the interference area at the time of osteotomy, a 3D modeling program is used to design the osteotomy guide and then it was printed using 3D printer. The osteotomy guide was fixed to a phantom skull, and Le Fort I osteotomy was performed along the designed osteotomy line. After surgery, the CBCT data of the skull model is acquired and the accuracy of the positioning of the

guided osteotomy line is evaluated by superimposing the preoperative virtual 3D model on the postoperative 3D CBCT. Subsequently, guide template is fitted to the skull model using sticky wax and images were acquired with a laser model scanner before and after screw fixation of the template on the maxilla surface. The accuracy of guide positioning was evaluated by superimposing the laser scanned image and the pre-operative (T0) virtual guide image in a 3D analysis program.

.

II. A new method of repositioning the osteotomized maxilla to planned position using a 3D position recognizing function of robot and a navigation system under movable head position is developed. This system is consisted of a robot-arm with seven degree of freedom (LBR iiwa, KUKA, Germany), a head registration zig, an image-guided navigation system (including an optical tracking camera and tracking tool), a display and a PC.

The navigation system uses an optical tracking system (POLARIS SPECTRA, Northern Digital Inc., Ontario, Canada) and simultaneously tracks the reflection body of skull head and the wafer for maxilla. First, the head registration zig that can be gripped by a robot end-effector was made using CAD / CAM technology, and the zig was attached to the upper side of the right supraorbital ridge. The preoperative head position was registered when the robot end effector was connected to the

head registration zig. Conventional Le Fort I osteotomy was performed along the osteotomy line of the pre-fabricated guide template. After separation of the upper and lower part, the skull was moved to the preoperative original position using the head registration zig and stored position of the robot. The accuracy of returning process of the head position to the preoperative location was evaluated by intraoperative navigation system. After registration of head position, the robot arm is connected to the wafer for the maxillary repositioning, and the robot arm is moved by the surgeon's hand as close to the planned position as possible while watching the real-time navigation images on the display. Then, we moved the maxillomandibular complex to the final position (in the sub-millimeter scale) using a smart pad. Preoperative CBCT images (TO) and postoperative CBCT images (T1) were used to evaluate the accuracy of the system.

Results

I. Deviation of the osteotomy guide was evaluated by comparing 8 landmarks on the guide template of a 3D virtual model and the laser scanned data of the actual 3D printed guide. RMSD (Root mean square deviation) was 0.85 ± 0.24 mm before fixation and 0.64 ± 0.19 mm after fixation.

The positional differences between the planned and actual 4-osteotomy lines were calculated using a wall thickness analysis function in a 3D CAD program. The mean difference was 0.49 ±

0.33 mm for the upper line, 0.56 ± 0.23 mm for the lower line and 0.48 ± 0.23 mm for the all lines.

II. The discrepancy between the original position and returned position of the phantom skull head was evaluated using the intraoperative navigation system. The RMSD between the original and returned position was 0.37 ± 0.44 mm over 12 experiments

Mean absolute deviations on all landmarks in manual repositioning to planned position were 0.59 ± 0.36 mm in mesio-lateral direction, 0.89 ± 0.62 mm in antero-posterior direction, and 0.53± 0.36 mm in supero-inferior direction, and when using smart pad, mean absolute deviations were 0.35 ± 0.27 mm in mesio-lateral direction, 0.48 ± 0.24 mm in antero-posterior direction, and 0.42 ± 0.40 mm in supero-inferior direction. The RMSD was 1.34 ± 0.50 mm by manual mode and 0.84 ± 0.48 mm by smart pad.

During the stabilization of the maxilla with L-shape plates, maxillary segment was moved slightly to 0.32 ± 0.21 mm in medio-lateral direction 0.27 ± 0.25 mm in antero-posterior direction, 0.42 ± 0.32 mm in supero-inferior direction compared with before the stabilization of the maxilla.

At the end, we compared the planned location of virtual maxilla with the actual post-operative 3D CBCT image. The RMSD between planned and actual postoperative maxillary

position was 1.22 ± 0.47 mm .

Conclusions

We developed new methods for maxillomandibular complex repositioning to the planned position under movable head condition using a robot with the 3D position recognizing function and a navigation system. The results confirmed that this system showed clinically satisfactory levels of maxillary repositioning even when a patient's head was moving. We also designed the new osteotomy guide template positioned precisely on planned positions and helped to quickly reposition the maxillomandibular complex to target positions for robot-assisted and navigation-assisted orthognathic surgery.

Keywords: orthognathic surgery, osteotomy guide, robot, 3D printing, 3D position recognizing function, navigation system, accuracy

Student Number: 2013-31193

CONTENTS

INTRODUCTION

MATERIALS AND METHODS

PART I. OSTEOTOMY GUIDE-BASED LEFORT I OSTEOTOMY

A. Design of the CAD/CAM-based osteotomy guide

B. Accuracy of the CAD/CAM-based osteotomy guide positioning

1. Deviation of the CAD/CAM-based osteotomy guide

2. Accuracy of the location of the guided osteotomy line

C. Statistical analysis

PART II. ROBOT WITH THE 3D POSITION RECOGNIZING FUNCTION AND NAVIGATION SYSTEM ASSISTED ORTHOGNATHIC SURGERY UNDER MOVABLE HEAD POSITION

A. System

B. Work flow

1. Preoperative phase

2. Intraoperative phase

C. Evaluation of the accuracy

D. Statistical analysis

RESULTS

PART I. OSTEOTOMY GUIDE-BASED LEFORT I OSTEOTOMY

A. Deviation of the CAD/CAM-based osteotomy guide

B. Accuracy of the location of the guided osteotomy line

PART II. ROBOT WITH THE 3D POSITION RECOGNIZING FUNCTION AND NAVIGATION SYSTEM ASSISTED ORTHOGNATHIC SURGERY UNDER MOVABLE HEAD POSITION

A. Evaluation of the accuracy of head positioning to its original position after surgery using the 3D position recognizing function of the robot

B. Comparing accuracy of maxilla repositioning between manual mode by hands and using smart pad

C. Evaluation of the accuracy of the maxillary repositioning in the changed head position using navigation system

D. Comparison of planned location of maxilla from virtual surgery and actual surgery using CBCT

DISCUSSION

CONCLUSION

REFERENCES

TABLES

FIGURES

ABSTRACT IN KOREAN

Development of repositioning method of maxillomandibular complex under movable head position using robot with the 3D position recognizing function and navigation system in orthognathic surgery

Jae Bong Park, D.D.S., M.S.D.

Program in Oral and Maxillofacial Surgery, Department of Dental Science, Graduate School, Seoul National University

(Directed by Professor Soon Jung Hwang, Dr. med. Dr. med. Dent)

INTRODUCTION

In the past, a surgical plan for orthognathic surgery was established mainly based on a clinical evaluation that includes, two dimensional (2D) -cephalometric analysis, and clinical photographs. As the accessibility of CT increases and the performance of three dimensional (3D) simulation programs increases, surgical plans based on 2D cephalometric prediction have been gradually replaced by 3D simulation surgery[1-5]. With development of three-dimensional (3D) CT and 3D simulation

program, surgical outcomes can be predicted in advance, making it possible to establish a more reliable surgery plan. Moreover, errors in model surgery and fabrication of acrylic splints could be avoided by 3D printing of an intermediate splint based on 3D virtual surgery[1,6-10]. However, even with a 3D simulation surgery and 3D printed intermediate splint, there are still several problematic procedures, which can reduce the surgical accuracy of simulation surgery. These include: (i) registration of centric occlusion - centric relation discrepancy, (ii) a variable condylar rotation center and movement during perioperative mandibular autorotation for maxillary repositioning with intermediate splint, (iii) changes in condylar position in case of centric occlusion - centric relation discrepancy under intraoperative muscle relaxant and (iv) changes in patient posture in the real operation field[1,2,6,8,10,11]. These condyle related errors can be avoided only by independent maxillary repositioning without mandibular autorotation, and advances in computer-aided design /computer-aided manufacturing (CAD/CAM) and 3D printing technologies have provided a way to develop new surgical procedures for independent maxillary repositioning [1-5].

In orthognathic surgery, instead of intermediate splints for the repositioning of maxillary segments, various forms of template or patient-specific implants based on maxillary occlusal surfaces or maxillary 3D surface topography were

designed and fabricated by 3D printing or CAD/CAM to guide Le Fort I osteotomy and to reposition the maxillary segment or maxillomandibular complex, and these clinical results were successful [1,2,7,9,12-18].

The templates or patient-specific implant based maxillary surgery has several shortcomings. Maxillary periosteum should be widely detached for insertion and placement, and it cannot be properly used in patients with a short midface and thin maxillary bone. Moreover, maxillary vertical position in the preoperative surgical plan is usually determined by incisal exposure after the predicted soft tissue changes based on the maxillary movements. However, the soft tissue prediction is still inaccurate even with 3D evaluation tools. While maxillary vertical position can be modified perioperatively by mandibular autorotation in the conventional methods with intermediate splint, it cannot be modified in the template based maxillary surgery because the template can provide guidance only on the predetermined unique maxillary position. In addition, the large volume of non-metal templates deforms midface soft tissue [1,12], which make it impossible to access soft tissue changes based on the maxillary movement. The other limitation is the difficulty in recognizing of residual bone interference between the osteotomized maxillary segment and skull part maxilla during installation on the maxillary surface. When the bone interference is located at the invisible maxillary posterior

region, pitch deviation can occur during repositioning due to the bending flexibility of the template, which can be difficult to recognize during surgery. Therefore, there is a tendency to over-resection the bone interference part to avoid bone interference. This can lead to little or no bone contact, and thus to postoperative instability.

The application of a navigation system that can track the location of the maxilla-mandibular complex in real time can provide 3D positional information of the complex, thus increasing the accuracy of surgical positioning of the complex. Several studies about navigation-guided maxillary positioning without an intermediate splint or templates have been reported with acceptable accuracies. However, this usually takes longer, and it is difficult to keep the adjusted position of maxillary segment manually during osteosynthesis even with the help of the navigation system, this is because of the plate bending inaccuracy and drilling error in addition to hand fatigue and tremors encountered while maintaining the position of the maxillary segment [19-21].

The previously mentioned methods for orthognathic surgery are based on a correct evaluation of a patient's status and the corresponding prediction with adequate treatment planning. However, soft tissue prediction based on jaw movement is still inaccurate, and facial asymmetry and profiles can be changed by head posture. Therefore, their preoperative assessments

can be wrong, which leads to inadequate surgical plans and simulations. If these conditions encountered perioperatively, the fabricated intermediated splint, maxillary template or patient specific implants are useless. To overcome these problems, a new approach is needed, which can provide leeway to change the operative plan.

Recently, robot assisted surgery has been applied in various surgical fields[22]. These robots perform minimally invasive surgery to reduce pain and complications and promote rapid recovery and short hospital stays. They can also overcome human physical limitations such as surgeon tremors or fatigue errors caused by prolonged surgery or degree of freedom and can enhance the surgeon's ability to manipulate tissue[23]. In orthognathic surgery, robot arm can be utilized for the repositioning of a maxillary segment or maxillomandibular complex without using a splint, which can eliminate procedural errors from traditional methods of using intermediate splints. Robot-assisted orthognathic surgery is able to change the surgical plan during surgery if the pre-operative preparation is inadequate.

Woo et al.[17] developed a method for automatically moving the maxilla to the planned position by synchronizing the robot arm, the navigation system and the 3D simulation program, and a clinically satisfactory study was published. However, since the robot arm does not have its own 3D position recognition

function, this is time consuming because it can move the osteotomized maxilla only through manual repetitive manipulation in the process of removing interference after a Le Fort I osteotomy.

In this study, we tried to develop a method for repositioning the maxillomandibular complex as planned before the surgery by using the robot's 3D position recognizing function and a navigation system that recognizes and reflects the change in position of the head during surgery. Then, for pre-clinical evaluation, we evaluated the validity and reliability of the system in various surgical plans using phantom skulls. Bony interference can occur in most of the maxillary repositioning, and removing this would be a time-consuming task in robot surgery. To reduce this inconvenience, we designed an osteotomy guide template for the Le Fort I osteotomy in this study. When the template is not fixed in the planned position, subsequent procedures including osteotomy, removal of bony interference, and repositioning of bony segments can differ from simulation. The final surgical outcome can also differ from the planned, predicted outcome. Therefore, we assessed the accuracy of positioning of the osteotomy guide, because placement of the guide in the same position as in simulation surgery is essential for precise subsequent surgical procedures.

MATERIALS AND METHODS

PART I. OSTEOTOMY GUIDE-BASED LEFORT I OSTEOTOMY

1. Design of the CAD/CAM based osteotomy guide

A total 12 phantom skull models (3B Scientific, Hamburg, Germany) were used for the study. They were divided into four groups according to surgical movement (Table 1). Preoperative 3D CBCT (DENTRI-2; HDXWILL, Korea) images were obtained under 80kVp and 10 mAs, and images were subsequently converted into STL files using MIMICS Software (Materialise, Leuven, Belgium). A 3D skull model was reoriented to a natural head position. We established a 3D coordinate system (X, Y, Z) (X, medio-lateral; Y, antero-posterior; Z, supero-inferior). The SN7 plane was 7 degrees less than the FH plane and was used as a horizontal reference plane, and the X-axis was set as the vector from the right to the left orbitale (Or). The midsagittal plane was defined as the plane perpendicular to the X-axis and passing through a nasion (N). The coronal plane was that which passed through the line passing the orbitale and perpendicular to the SN7 plane.

A Le Fort I osteotomy and BSSRO were performed using the program (Mimics, Materialise, Leuven, Belgium) and the osteotomized maxillomandibular complex was moved according to the treatment plan. As the maxilla segment was repositioned, a collision occurred between the two bony segments. A simulation program was used to identify these interferences

and an osteotomy guide was made to remove these interferences simultaneously during osteotomy (Figure 1). A total of four osteotomy lines, two upper and two lower, were vertically reinforced so that they can be guided to an angle as well as the direction of the reciprocating saw. To maximize the accuracy of template fitting, a template was designed to cover the characteristic 3D surfaces and curvatures of the maxilla, such as the piriform aperture, anterior maxillary wall including canine eminence, zygomaticomaxillary buttress, and anterior nasal spine. The lower part included one-third of the piriform aperture to the anterior nasal spline and maxillary frontal wall from the canine eminence to the posterior part. The upper part contained the middle portion of the piriform aperture, up to below the infraorbital foramen and laterally to the zygomaticomaxillary buttress. To reduce pre-operative preparation time, the upper and lower parts were connected to a 2-mm thin bridge on the mesial side to simplify the design and two drill holes were made to stabilize the guide template. All designed templates were fabricated using a 3D-printing technique and were sterilized (Cubicon Single Plus, Cubicon, Korea). The 3D-printed osteotomy guide was placed on the surface of the phantom skull and fixed it with 8 mid-screws in 1.6-mm-diameter drill holes (Figure 2). Le Fort type 1 osteotomy was performed along the osteotomy line of the guide template. After the lower part of the maxilla with a robot arm

was separated from the upper part by hand, interference was removed with a round bur. We stabilized the osteotomized maxilla using four L-shaped, four-hole miniplates on the piriform aperture and zygomatic buttress area and performed a CBCT scan. CBCT data of skull models were acquired after surgery (T1) and the accuracy of the osteotomy line was evaluated by superimposing the final 3D CBCT (T1) image and the 3D skull image that underwent virtual surgery preoperatively (T0). Images were acquired with a laser model scanner before and after screw fixation of the template on the maxilla surface. The accuracy of guide positioning was evaluated by superimposing the laser scanned image and the pre-operative (T0) virtual guide image in a 3D analysis program (3-Matic, Materialise, Leuven, Belgium).

2. Accuracy of the CAD/CAM-based osteotomy guide positioning

To evaluate the accuracy of osteotomy guide positioning, 3D CBCT, a laser scanner (Identica Blue, Medit, Seoul, Korea), and a 3D CAD program were used. To evaluate the deviation of the surgical template, we added 8 cone-shaped reference structures (4 on each of the right and left parts) on the template. A 3D-printed osteotomy guide was placed and fixed with 8 midscrews on the anterior maxilla of phantom skull, and Le Fort I osteotomy was performed. After surgery, CBCT scan

data (T1) were acquired to compare the actual location of the osteotomy line with the planned location in simulation surgery. Subsequently, a laser scan (Identica Blue, Medit, Seoul, Korea) of the guide template fixed to the osteotomized maxilla was also acquired to compare the actual and planned positions.

Deviation of the CAD/CAM-based osteotomy guide

To evaluate deviations of the 3D-printed osteotomy guide, we compared the virtual osteotomy guide and the laser scanned actual osteotomy guide (Figure 3). First, 3D CBCT data of the maxilla at T0 with the virtual osteotomy guide and laser scan data of the osteotomy guide with osteotomized maxilla after surgery were imported into a 3D-analysis program (3-Matic, Materialise, Leuven, Belgium). Based on the unchanging maxilla dentition, superimposition of the two 3D images was performed with point and global registration function[24]. The absolute deviations of three-dimensional positions of the 8 cone-shaped reference structures were measured between virtual and actual osteotomy guides.

Accuracy of the location of the guided osteotomy line

To assess the accuracy of osteotomy guide positioning on the maxilla of phantom skulls, CBCT images from T1 were imported into Mimics software (Materialise, Leuven, Belgium) to compare the position of the osteotomy line relative to the

pre-operative simulation position (Figure 4). Planned and actual osteotomized maxilla upper and lower parts were superimposed in the simulation program, and overlapping parts were removed using a Boolean function. The remaining portion of the maxillary front wall was subjected to wall thickness analysis in the 3-matic CAD program (Materialise, Leuven, Belgium).

4. Statistical analysis

Statistical analysis was performed using SPSS version 25.0 (SPSS Inc., Chicago, IL, USA). Data were tested for normality using the Kolmogorov-Smirnov test, and a nonparametric test was used. To evaluate the accuracy of positioning of the osteotomy guide, Wilcoxon signed-rank tests were performed for x-, y- and z coordinates between the planned and actual images. Absolute deviations in medial-lateral, anterior-posterior, and superior-inferior directions were assessed, and the 3D distance of the reference structure between planned and actual positions of landmarks was calculated using the root mean square deviation (RMSD) formula. The level of significance was set at $p < 0.05$. To evaluate differences in the accuracy of the location between the upper osteotomy line and the lower osteotomy line, Mann-Whitney U tests were performed. The level of significance was set at $p < 0.05$.

PART II. ROBOT WITH THE 3D POSITION RECOGNIZING FUNCTION AND NAVIGATION SYSTEM ASSISTED ORTHOGNATHIC SURGERY UNDER MOVABLE HEAD POSITION

1. System

This system is consisted of a robot-arm with seven degree of freedom (LBR iiwa, KUKA, Augusburg, Germany), head registration zig (H-zig), an image-guided navigation system including an optical tracking camera and tracking tool, PC and monitor (Figure 5). The robot-arm is controlled by the smart pad provided by the manufacturer, and the repeatability and maximum payload of the robotic system were ± 0.1 mm and 7 kg, respectively. The jog mode can move the robot by hand while push the specific button on the flange. The velocity of the jog cannot exceed 250 mm/s and can be set in steps to the following values: 100%, 75%, 50%, 30%, 10%, 5%, 3%, 1%, 0%. It has 3-dimensional position recognizing function, so it is possible to return to the original position by pushing the button on the smart pad after manually teaching the robot arm a specific position and storing it.

The tool that can move the osteotomized maxillomandibular complex is designed with maxillary positioning splint (MxP-spint) and connector that can be gripped by the end effector of the robot (Figure 6-7). A virtually osteotomized maxilla 3D

image was imported into the 3D modeling program as a STL file. The virtual horseshoe shape 3D mold was created to be about one-third the height of the tooth using program. Then, using a subtraction function called Boolean, the virtual splint of the maxillomandibular dentition was designed and fabricated by 3D printing. The MxP-splint connector was also fabricated using CAD / CAM.

To reflect the change in the head position during the operation, the skull model was fixed semi-rigidly on the heavy steel plate using a camera tripod head. The robot was placed on the left side of the skull, considering that the operator is generally located on the right side of the patient. Before surgery, the surgeon evaluates the patient's facial appearance, and if the position of the head changes during or after surgery, different results can be obtained each time. To overcome this limitation, a head registration zig was created to store 3D coordination of the preoperative head position. Using a 3D modeling program and 3D printer, a head registration zig (H-zig) that can be gripped by a robot end effector is designed and fixed to the right upper area of the supra orbital ridge of the phantom skull. H-zig and the position recognizing function of the robot can save the position of the head before the surgery and can move the skull head to the stored position at any time during the operation or at the end of the operation. The navigation system uses an optical tracking system

(POLARIS SPECTRA, Northern Digital Inc., Ontario, Canada) and simultaneously tracks the reflection body of the skull model and the wafer. The planned and the actual maxillomandibular position information are visualized on the PC monitor of the navigation system in real time. The amount of deviation is visualized in real time on eight landmarks, including the incisal edges of incisors, canines, mesio-buccal cusp of the maxillary first molars, and pogonion.

2. Work flow

A flowchart of robot assisted and navigation system assisted orthognathic surgery is shown in figure 8.

Preoperative phase

A LEGO block (LEGO Group, Billund, Denmark) is placed on the upper left of the supra orbital ridge of the phantom skull to mount the registration body. For registration between 3D virtual space and actual physical space, the registration body was connected to the wafer with a LEGO block, and it was designed to have eight holes with 1 mm-stainless steel spheres for use as registration fiducial markers (Figure 9)[17,20,25-27]. The MxP splint with the registration body was fixed to the maxillary teeth of the skull using sticky wax. Then CBCT (DENTRI-2; HDXWILL, Korea) images were acquired under 80kVp and 10m using a thickness slice of 0.20 mm. The actual space is

synchronized to the space of the CBCT data by using a registration marker. After taking CBCT data, a virtual 3D model was constructed. A Le Fort I osteotomy was performed using Mimics Software (Materialise NV, Leuven, Belgium) according to the 4 surgical plans and then the osteotomized maxilla was moved to the planed position.

The actual positions of fiducial markers on the registration body were measured using a tracking tool tip (Northern Digital Inc., Ontario, Canada) for registration to their corresponding spheres on the 3D CBCT space.

Intraoperative phase

After the phantom skull was semi-rigidly fixed to the steel plate to reflect the change of the patient's head position condition, the direction of the phantom skull was changed to a position where the surgeon was comfortable manipulating it. Using the jogging mode, the robot arm was moved to the H-zig manually, and it was held with the end effector using a smart pad. The 3D position of the phantom skull was stored using the 3D position recognition function (Figure 10). Then, the registration body was attached to the same position as the 3D CBCT (T0) model for registration between the 3D virtual space and actual space, and a reflection body was attached to the head and MxP splint using LEGOs. Each of them were tracked to record the relative position immediately before the surgery and

to observe the position change in real time during the operation. After registration, a Le Fort I osteotomy was performed according to the osteotomy line of the pre-fabricated osteotomy guide, and both upper and lower parts were separated. Before repositioning the osteotomized maxilla, the semi-rigidly fixed phantom skull head was manually moved to the pre-operative position. The robot arm was moved to the H-zig by the operator, then the H-zig was held using the end effector. The robot arm moved the head to the original position automatically using a 3D position recognition function, and it was fixed using a camera tripod screw. When the phantom skull head was positioned preoperatively, we removed the gripper from the H-zig and held the MxP-splint connector. Because the skull head and osteotomized maxilla were tracked using the navigation system, the maxillomandibular complex can reach the planned position while being visualized on the display. At first, the robot arm was manually held and moved as close as possible to the planned position while viewing the display screen (Figure 11). Then, the maxillomandbular complex was moved to the planned position by x, y, z, pitch, rolling, yawing movement in sub-millimeter scales using smart pad. If a collision occurs due to the interference between the upper and lower bony segment, the robot will stop. At this time, the interference can be identified by eye, and the current coordinates can be stored. After the lower part of the maxilla

(with the robot arm) is separated from the upper part by hand, interference is removed with a round bur, and the arm is returned to the stored coordinates automatically. This process is repeated several times, then the arm becomes as close as possible to the planned position. We fixed the lower osteotomized maxilla to the upper part using four L-shaped four-hole miniplates near both the piriform aperture and zygomatic buttress area and conducted a CBCT scan (Figure 12).

3. Evaluation of the accuracy

A total of 12 experiments with four different surgical plans were performed and each surgical plan was conducted three times. We used the H-zig and the position recognition function of the robot to return the skull head to its original position during the clinical evaluation of a patient's face before surgery, intraoperatively, and after surgery in the same conditions. The navigation system was used to track the reflection body of the head and evaluate the accuracy of this head returning process.

According to the surgical plan, maxillary Le Fort I was performed following the intraoperative work flow. The difference in accuracy of the manual movement of the robot arm and the movement of the robot arm with the smart pad was evaluated. After surgery, postoperative CBCT images (T1) were obtained to analyze the postoperative maxillary position.

Since the CBCT data of the phantom skull is low in resolution and it is difficult to evaluate the accuracy when the landmark of the tooth and, optical scan data of the cast model are obtained using a laser scanner (Figure 13). Laser scanned dentition is registered in the dentition of the planned 3D skull model and the dentition of the postoperative 3D skull model using a point and global registration function. Planned and postoperative 3D skull models merged with laser scanned dentition were imported into 3D CAD software (3-Matic, Materialise NV, Leuven, Belgium). Since the same scan data of the dental cast were used to register the pre-operative and post-operative 3D skull models, we can make a precise comparison by taking a point at the same position.

The difference in the accuracy of maxilla repositioning when using the manual mode and using the smart pad before and after fixation of the osteotomized maxilla were measured using the intraoperative navigation system on seven landmarks. These included the incisal edges of incisors, canines, the mesio-buccal cusp of the maxillary first molars and the pogonion.

4. Statistical analysis

Statistical analysis was performed using SPSS version 25.0 (SPSS Inc., Chicago, IL, USA). The normality of the data was tested using the Kolmogorov-Smirnov test. First, the accuracy of the head positioning was evaluated using the changes in

coordinates in the x−, y− and z− axis and RMSD. Second, the accuracy of the maxillary repositioning was evaluated using the changes in coordinates in the x−, y− and z− axis and RMSD. The Wilcoxon signed−rank test was performed to assess the significance of the differences between paired data. Then, the mean difference between the manually and smart pad derived position of the maxilla and planned− and actual position of the maxilla was described based on the mean value and standard deviation.

RESULTS

PART I. OSTEOTOMY GUIDE−BASED LEFORT I OSTEOTOMY

A. Deviation of the CAD/CAM−based osteotomy guide

Deviation of the osteotomy guide was evaluated by comparing 8 landmarks on the guide template of a 3D virtual model and the laser−scanned data of the actual 3D−printed guide. Mean absolute deviations based on the 8 reference landmarks of 12 osteotomy guides before and after stabilization to the maxilla surface are shown in Table 2, 3. Mean absolute deviation was 0.17 ± 0.12 mm in the medial−lateral direction; before fixation, the values were 0.71 ± 0.28 mm in the anterior−posterior direction, 0.32 ± 0.23 mm in the superior−inferior direction, and 0.26 ± 0.20 mm in the medial−lateral direction; the values

after fixation were 0.41 ± 0.20 mm in the anterior−posterior direction and 0.30 ± 0.20 mm in the superior−inferior direction. RMSD was 0.85 ± 0.24 before fixation and 0.64 ± 0.19 after fixation. Statistically significant differences were observed after fixation ($p = 0.000$)

B. Accuracy of the location of the guided osteotomy line

The positional differences between the planned and actual osteotomy lines were calculated using a wall thickness analysis function in a 3D CAD program (Table 4). To compare the positional accuracy of upper and lower parts of the osteotomy guide, where the four lines were divided into an upper line group and a lower line group. The mean difference was 0.49 ± 0.33 mm for the upper line, 0.56 ± 0.23 mm for the lower line, and 0.48 ± 0.23 mm for all lines. Differences between upper and lower lines were not significant ($p = 0.133$).

PART II. ROBOT WITH THE 3D POSITION RECOGNIZING FUNCTION AND NAVIGATION SYSTEM ASSISTED ORTHOGNATHIC SURGERY UNDER MOVABLE HEAD POSITION

A. Evaluation of the accuracy of head positioning to its original position after surgery using the 3D position recognizing function of the robot

The navigation system was used to track the reflection body of the head and evaluate the accuracy of the head returning process. The mean registration error of the navigation system was 0.38 ± 0.06 mm (Table 5). Discrepancies between the stored and returned position of the skull head were evaluated (Table 6). The mean absolute discrepancies with respect to the 3D coordination system of the reflection body on the skull head were 0.19 ± 0.27 mm in the medio-lateral direction, 0.14 ± 0.22 mm in the antero-posterior direction and 0.24 ± 0.30 mm in the supero-inferior direction, 0.016 ± 0.132 mm in degrees of yaw, 0.0025 ± 0.002 mm in degrees of pitch, and 0.0174 ± 0.019 mm in degrees of roll. The RMSD was 0.37 ± 0.44 mm between the original and returned position in 12 experiments.

B. Comparing accuracy of maxilla repositioning between manual mode by hands and using smart pad

Mean absolute deviations on all landmarks in manual repositioning to the planned position were 0.59 ± 0.36 mm in the mesio-lateral direction, 0.89 ± 0.62 mm in the antero-posterior direction, and 0.53± 0.36 mm in the supero-inferior direction, and when using smart pad mean absolute deviations were 0.35 ± 0.27 mm in mesio-lateral direction, 0.48 ± 0.24 mm in antero-posterior direction, and 0.42 ± 0.40 mm in supero-inferior direction (Table 7, 8). Statistically, there was a significant difference in the accuracy of the manual mode and

smart pad in all directions (p=0.000 in the mesio-lateral direction, antero-posterior direction and p=0.009 in the supero-inferior direction). The RMSD was 1.34 ± 0.50 mm for the manual mode and 0.84 ± 0.48 mm for the smart pad. There were statistically significant differences in RMSD between the manual mode and smart pad (p=0.000)

C. Evaluation of the accuracy of the maxillary repositioning in the changed head position using navigation system

Mean absolute deviations on all landmarks before fixation were 0.35 ± 0.27 mm in the mesio-lateral direction, 0.48 ± 0.24 mm in the antero-posterior direction, and 0.42 ± 0.40 mm in the supero-inferior direction compared with planned position (Table 9). We also evaluated the maxillary position after fixation using intraoperative navigation. Compared with the planned position, mean absolute deviations of all landmarks were 0.40 ± 0.37 mm in the medio-lateral direction, 0.57 ± 0.47 mm in the antero-posterior direction and 0.50 ± 0.39 mm in the supero-inferior direction. The RMSD difference between the planned position and position after fixation was 0.99 ± 0.52 mm, and there were statistically significant differences in RMSD during fixation (p=0.002) (Table 10).

During the stabilization of the maxilla with L-shape plates, the maxillary segment was moved slightly to 0.32 ± 0.21 mm in the medio-lateral direction 0.26 ± 0.27 mm in the antero-

posterior direction, and 0.42 ± 0.32 mm in the supero-inferior direction compared with before the stabilization of the maxilla (Table 11).

D. Comparison of planned location of maxilla from virtual surgery and actual surgery using CBCT

At the end, we compared the planned location of the virtual maxilla with the actual post-operative 3D CBCT image (Table 12, 13). The mean absolute discrepancy with respect to the location of the landmarks was 0.45± 0.36 mm in the medio-lateral direction, 0.87 ± 0.50 mm in the antero-posterior direction and 0.46 ± 0.38 mm in the supero-inferior direction. The RMSD was 1.22 ± 0.47 mm between the planned - and actual postoperative maxillary position.

DISCUSSION

Over a long period of time, oral and maxillofacial surgeons have investigated how to accurately reposition the maxillomandibular complex to a planned position. In conventional orthognathic surgery, oral and maxillofacial surgeons use an intermediate splint with mandible autorotation for maxillary repositioning. However, malposition of the condyle and surrounding tissue can occur during surgery, so it is still very difficult to accurately transfer a surgery plan to the

operation field[19]. In addition to this error, there are several procedures that decrease accuracy during preparation of the orthognathic surgery, including impression, making a cast model, face bow transfer, model surgery and fabrication of acrylic splints. Advances in CAD/CAM and 3D-printing technologies have developed and provided adequate information for repositioning of maxillomandibular complex to overcome many errors [26,28-30]. Many CAD / CAM based templates have been developed to overcome the inaccuracies of the intermediate occlusal splint based orthognathic surgery. The CAD/CAM based template uses a maxilla dentition or three-dimensional curvature of the maxillary surface of 3D virtual skull models generated from CT data to eliminate the errors caused by autorotation of condyle and face-bow transfer. However, the template' s large volume causes nerve damage due to large exposure, making it impossible to assess changes in facial soft tissue due to the great lip distortion. In addition, the accuracy of the maxilla repositioning may be degraded due to the deformation of the template during the collision between the upper part and lower part of the maxilla. Both conventional orthognathic surgery and template-based orthognathic surgery provide less flexibility for additional perioperative changes in the surgical plan[1]. Therefore, it is necessary to develop a new surgical method that can change the plan during surgery [1,13,14].

Real-time navigation systems were also designed to verify

that the complex was positioned as planned during surgery and available if the surgical plan needs to be changed during the operation. This system obtains CBCT images that have been obtained during preoperative virtual surgery; these register the intraoperative position of the patient's head and maxillomandibular complex with the virtual image using the optical tracking system or electromagnetic system. Then, the system checks the position in real time. The accuracy of navigation system for orthognathic surgery has been reported by several researchers. Chapuis et al.[19] performed the Le Fort I osteotomy and tracked the position of osteotomized maxilla using an optical tracking system. They reported an accuracy of 1.1 mm between planned and postoperative skull models based on the maxilla bone surface. Lee et al.[20] repositioned the virtual maxillo-mandibular complex using an optical tracking system. Their RMSD between the planned and intraoperative guidance stages were 0.23 ± 0.09 mm, 1.03 ± 0.19 mm, and 0.47 ± 0.27 mm on the x-, y-, and z-axes, respectively. The mean RMS deviation was 1.16 ± 0.34 mm for eight maxillary teeth and one mandibular pogonion (Pog) landmark. In the evaluation of the postoperative results using CT data, the RMSD was 1.31 ± 0.28 mm for maxillary landmarks. In another study that employed an electromagnetic navigation system[21], the mean absolute deviation between the planned- and actual maxillary positions were 0.8 mm in the x-axis, 2.2 mm in the y-axis and 1.3 mm

in the z-axis. The RMS was 2.8 mm. However, they reported that even with navigation equipment, manual repositioning and stabilization of the maxilla is time consuming and inaccurate and due to hand tremors [21].

To overcome these limitations, research has been attempted using a robot arm in conjunction with a navigation system. Robots are already widely used in laparoscopic and orthopedic fields, and minimally invasive surgery using robots leads to reduced pain and complications, rapid recovery, and short hospital stays. They can also overcome human physical limitations such as surgeon tremors or fatigue errors caused by prolonged surgery. Ali Uneri et al. developed a robot for vitreoretinal surgery[31], German Aerospace Center developed the robotic system, MiroSurge[32], for invasive telesurgery. And some representative such as da Vinci, ROBODOC, ACROBOT, etc. are already widely used. There have been few attempts to combine robotic technology with orthognathic surgery [33-36]. In orthognathic surgery, robots can act as intelligent assistants, performing relative repositioning of mobilized bone and holding bone segments in planned target positions during surgery[35]. Compared to previous studies that used only an optical tracking system to reposition the osteotomized maxilla, the accuracy of the maxillary repositioning was improved with the aid of a robotic arm specially designed for orthognathic surgery. Burgner et al.[34,35] developed an end effector and performed

robot and navigation assisted orthognathic surgery using a robot called RX 90 (Stäubli, Horgen, Switzerland) an optical tracking system. However, they did not use virtual surgery and a real-time display. Rather, they performed face bow transfer in a conventional way, and then moved the maxilla using splints with an end effector by the difference between the maxillary position before and after the model surgery. However, the accuracy of repositioning the maxilla after robot surgery was not evaluated. Viera et al.[36] evaluated the stability and usefulness of a light weight robot to hold the maxilla at target position while the surgeon drills and fixes the maxilla. The final position error for the original position was less than 0.01 mm, which was clinically viable. In a recent study, Wang et al.[33] developed a robotic system for orthognathic surgery using UR5 and a 3D navigation system. However, they carried out a preliminary experiment in which three distances between the references markers located in the lower part of the maxilla were measured after repositioning. Woo et al.[17] developed a method for automatically moving the maxilla to the planned position using a robot arm, a navigation system, and a 3D simulation program. Clinically satisfactory results were reported. The mean absolute differences were 0.33 ± 0.33 mm in the medio-lateral direction, 0.43 ± 0.3 mm in the antero-posterior direction, and 0.52 ± 0.51 mm in the supero-inferior directions respectively. The mean RMS difference was 0.87 ±

0.5 mm for the five teeth landmarks on the maxilla and the pogonion landmark on the mandible for 16 patients. However, because the procedure used for repositioning the osteotomized maxilla using robots and navigation is done while the skull is fixed, it is insufficient for clinical applications. In addition, since the robot arm does not have its own 3D position recognizing function, it takes a lot of time because the maxillary repositioning process has to start again from the beginning.

In contrast to Woo et al.'s study, we used the 3D position recognizing function of a robot-arm that stores the coordination of the 3D actual space where the TCP of the robot arm is located.

According to the manual provided by the manufacturer, the repeatability is about ± 0.1 mm. In this study, when the 3D position learning function was used to return the skull head to the preoperative position, the accuracy was assessed using the intraoperative navigation system and the mean RMSD was 0.37 ± 0.44 mm. This is somewhat larger than the repeatability of the robot itself, but there seems to be an additional error due to the experimental environment.

Preoperative virtual surgery, Le Fort I osteotomy and BSSRO should be performed for intraoperative registration and navigation guided maxillary repositioning. Then, the virtual osteotomized maxillomandibular complex was moved to the planned position to acquire the final position information of the

complex for navigation guided orthognathic surgery. In this process, the osteotomy line is set preoperatively, and the area that collides when the bony segments are moved according to the surgical plan can be confirmed in advance. Robot and navigation orthognathic surgery is more time consuming than conventional orthognathic surgery due to registration during surgery, connection and separation of bone fragments to the robot end effector and the process of removing the interferences during the repositioning of the maxilla. So, we designed and fabricated the osteotomy guide to reduce the time consuming steps.

Unlike conventional robotic arm studies, this study divided the maxillary repositioning into two stages, hand mode and smart pad mode. We then compared the results with the planned positions. When the maxillomandibular complex was moved by hand, the average RMSD was measured to be 1.34 ± 0.50, which was less accurate than that of Lee et al.'s study[20]'s study, wherein an RMS was 1.16 ± 0.34 mm measured by navigation alone without a robot. This is because the robot arm itself is heavy, even if the stiffness of the robot is reduced to a minimum, and it is impossible to control the robot in the sub-millimeter range. This results in frequent collision between the lower part and the upper part, and the position of the semi-rigidly fixed skull head was changed. After positioning the maxilla as close to the planned position as possible by hand, a

fine adjustment was made using a smart pad. The mean absolute deviations decreased when using a smart pad, providing statistically significant results in all directions.

When the robot was moved using the smart pad, shift movement was performed by setting the medio-lateral direction as the x-axis, the antero-posterior direction as the y-axis, and the suprero-inferior direction as the z-axis. Pitching and yawing movements were used to perform posterior impaction and yawing correction. A canting correction was made using the rolling movement of the seventh axis farthest from the robot base. The moving velocity was set at 3% or 1% of the maximum speed of 250 mm/s, and it was moved to the planned position by pushing the button for as short a time as possible. As expected, the accuracy increased significantly with the smart pad rather than the manual mode (medio-lateral: $p=0.000$, antero-posterior: $p=0.000$, supero-inferior: $p=0.009$ and RMSD: $p=0.000$). However, this result indicates somewhat more error than that of Han et al[27], which can be assumed to be an increase in errors due to the head movenment in this study. During the stabilization of the maxilla with L-shape plates, the maxillary segment was moved slightly to 0.32 ± 0.21 mm in the medio-lateral direction 0.27 ± 0.25 mm in the antero-posterior direction, and 0.42 ± 0.32 mm in the supero-inferior direction compared with before the stabilization of the maxilla. The reason for this increase is that the skull head is moved

slightly and the plate bending is not complete when the drilling is performed on the upper part of the maxilla. Thus, the skull is moved while the osteotomized maxilla is fixed. In the evaluation of actual surgery using postoperative CBCT data, absolute mean deviations mild increased by 0.10 mm in the medio-lateral direction , 0.39 mm in the antero-posterior direction, and 0.23 mm in RMSD compared with the accuracy evaluated using intraoperative navigation after fixation of the maxilla. These results are consistent with other previous studies [17,26]. In the supero-inferior direction, however, it decreased by 0.04 mm. Similar to this study, several studies reported an increase in RMSD based on a comparison of values immediately after maxilla stabilization and the postoperative results from CT data[20,21,27] This difference can be attributed to the error of the navigation system in registering the actual space and the virtual space, or the matching error between the dentition of the 3D CBCT images and the dentition of the laser scanned image. In this study, the mean registration error of the navigation system was 0.38 ± 0.06 mm. There is also error in the CBCT evaluation. First, since each slice has a thickness of 0.2 mm, the reconstructed 3D model may differ from the actual skull. We have set the tip of 6 teeth as landmarks for evaluation of accuracy, but the resolution of the CBCT image is low, and we cannot use the same spots. Therefore, the same laser scanned dentition was superimposed on both 3D CBCT images

to spot the exact same position in the preoperative and postoperative 3D CBCTs.

For intraoperative registration and navigation-guided maxillary repositioning, preoperative virtual surgery, Le Fort I osteotomy, and BSSRO should be performed. Then, the virtual osteotomized maxillomandibular complex is moved to the planned position to acquire final position information of the complex for navigation-guided orthognathic surgery. In this process, the osteotomy line is set preoperatively, and the area that collides when bony segments are moved according to the surgical plan can be confirmed in advance. Robot- and navigation-assisted orthognathic surgery such as registration during surgery, connection and separation of bone fragments to the robot end effector, and removal of interferences during repositioning of the maxilla are more time-consuming than in conventional orthognathic surgery. Therefore, if a guide is produced using collision information that can be confirmed during the preoperative simulation process, surgery time can be reduced. Kang et al.[37] designed an osteotomy guide template for surgery. The accuracy of the osteotomized maxilla was evaluated by comparing CT before and after surgery, but without quantitative analysis or evaluation of guide positioning accuracy. To accurately remove interferences, templates must be in the same position as in simulations; otherwise, the osteotomy position or removal of interference may differ from

simulation results and final results differ from the plan. Han et al.[27] produced a CAD/CAM-based template for osteotomy and repositioning. Similar to our study, they evaluated positioning accuracy using landmarks on the osteotomy guide; mean absolute deviation was 0.40 mm in the medial-lateral direction, 0.60 mm in the anterior-posterior direction, 0.7 mm in the superior-inferior direction; RMSD was 1.1 mm, similar to our findings of 0.26 mm on the x-axis, 0.41 mm on the y-axis, and 0.60 mm on the z-axis with RMS 0.64 mm. However, the accuracy was evaluated by positioning with adhesive and without screw fixation and did not reflect an actual surgical situation. In our study, the difference in position of the osteotomy line between the actual and virtual models was compared using wall-thickness analysis. To minimize preparation time with a simple design, the upper and lower parts of the guide template were designed to be connected with the bridge. The position accuracy of the upper part with the relatively small maximal contact area was expected to be low, but no significant difference was observed.

CONCLUSIONS

In this study, we designed a new osteotomy guide for robot-assisted orthognathic surgery The templates provided information about the osteotomy line and bony interference. An evaluation of positioning accuracy showed that the templates

had precise positioning (RMSD, 0.64 mm). The reproducibility of the location of the osteotomy line (mean 0.48 ± 0.23 mm) showed high accuracy. These results suggest that our CAD-CAM-based osteotomy templates could be positioned as planned and helped to reposition the maxillomandibular complex to the target position for robot-assisted and navigation-assisted orthognathic surgery.

In part II, We developed a new method for maxilla repositioning under a movable head position using the 3D position recognizing function of robot-arm and navigation system. We also fabricated a head registration zig (H-zig), a maxilla positioning splint (MxP-splint) and a MxP-splint connector for our research. The results of this study confirmed that the use of the 3D position recognizing function of the robot arm and navigation system can produce a clinically satisfactory level of maxillary repositioning even when a patient's head is moving (RMSD: before fixation 0.84 mm, after fixation: 0.99 mm, and postoperative CBCT: 1.22 mm).

REFERENCES

1. Han JJ, Yang HJ, Hwang SJ. Repositioning of the Maxillomandibular Complex Using Maxillary Template Adjusted Only by Maxillary Surface Configuration Without an Intermediate Splint in Orthognathic Surgery. *J Craniofac Surg.* 2016;27(6):1550-1553.
2. Zinser MJ, Sailer HF, Ritter L, Braumann B, Maegele M, Zoller JE. A paradigm shift in orthognathic surgery? A comparison of navigation, computer-aided designed/computer-aided manufactured splints, and "classic" intermaxillary splints to surgical transfer of virtual orthognathic planning. *J Oral Maxillofac Surg.* 2013;71(12):2151 e2151-2121.
3. Aboul-Hosn Centenero S, Hernandez-Alfaro F. 3D planning in orthognathic surgery: CAD/CAM surgical splints and prediction of the soft and hard tissues results - our experience in 16 cases. *J Craniomaxillofac Surg.* 2012;40(2):162-168.
4. Chen X, Li X, Xu L, Sun Y, Politis C, Egger J. Development of a computer-aided design software for dental splint in orthognathic surgery. *Sci Rep.* 2016;6:38867.
5. Li B, Wei H, Zeng F, Li J, Xia JJ, Wang X. Application of A Novel Three-dimensional Printing Genioplasty Template System and Its Clinical Validation: A Control Study. *Sci Rep.* 2017;7(1):5431.
6. Ellis E, 3rd. Accuracy of model surgery: evaluation of an old technique and introduction of a new one. *J Oral Maxillofac Surg.* 1990;48(11):1161-1167.
7. Li B, Zhang L, Sun H, Yuan J, Shen SG, Wang X. A novel method of computer aided orthognathic surgery using individual CAD/CAM templates: a combination of osteotomy and repositioning guides. *Br J Oral Maxillofac Surg.* 2013;51(8):e239-244.
8. Olszewski R, Reychler H. [Limitations of orthognathic model surgery: theoretical and practical implications]. *Rev Stomatol Chir Maxillofac.* 2004;105(3):165-169.
9. Bai S, Shang H, Liu Y, Zhao J, Zhao Y. Computer-aided design and computer-aided manufacturing locating guides accompanied with prebent titanium plates in orthognathic surgery. *J Oral Maxillofac Surg.* 2012;70(10):2419-2426.
10. Kahnberg KE, Sunzel B, Astrand P. Planning and control of vertical dimension in Le Fort I osteotomies. *J Craniomaxillofac Surg.* 1990;18(6):267-270.
11. Ferguson JW, Luyk NH. Control of vertical dimension during maxillary orthognathic surgery. A clinical trial comparing internal and external fixed reference points. *J Craniomaxillofac Surg.* 1992;20(8):333-336.
12. Suojanen J, Leikola J, Stoor P. The use of patient-specific implants in orthognathic surgery: A series of 32 maxillary

osteotomy patients. *J Craniomaxillofac Surg.* 2016;44(12):1913-1916.
13. Gander T, Bredell M, Eliades T, Rucker M, Essig H. Splintless orthognathic surgery: a novel technique using patient-specific implants (PSI). *J Craniomaxillofac Surg.* 2015;43(3):319-322.
14. Mazzoni S, Bianchi A, Schiariti G, Badiali G, Marchetti C. Computer-aided design and computer-aided manufacturing cutting guides and customized titanium plates are useful in upper maxilla waferless repositioning. *J Oral Maxillofac Surg.* 2015;73(4):701-707.
15. Polley JW, Figueroa AA. Orthognathic positioning system: intraoperative system to transfer virtual surgical plan to operating field during orthognathic surgery. *J Oral Maxillofac Surg.* 2013;71(5):911-920.
16. Brunso J, Franco M, Constantinescu T, Barbier L, Santamaria JA, Alvarez J. Custom-Machined Miniplates and Bone-Supported Guides for Orthognathic Surgery: A New Surgical Procedure. *J Oral Maxillofac Surg.* 2016;74(5):1061 e1061-1061 e1012.
17. Woo SY, Lee SJ, Yoo JY, et al. Autonomous bone reposition around anatomical landmark for robot-assisted orthognathic surgery. *J Craniomaxillofac Surg.* 2017;45(12):1980-1988.
18. Suojanen J, Leikola J, Stoor P. The use of patient-specific implants in orthognathic surgery: A series of 30 mandible sagittal split osteotomy patients. *J Craniomaxillofac Surg.* 2017;45(6):990-994.
19. Chapuis J SA, Pappas I, et al. A new system for computer-aided preoperative planning and intraoperative navigation during corrective jaw surgery. *IEEE Trans Inf Technol Biomed* 2007;2007;11:274-287.
20. Lee SJ, Woo SY, Huh KH, et al. Virtual skeletal complex model- and landmark-guided orthognathic surgery system. *J Craniomaxillofac Surg.* 2016;44(5):557-568.
21. Berger M, Nova I, Kallus S, et al. Can electromagnetic-navigated maxillary positioning replace occlusional splints in orthognathic surgery? A clinical pilot study. *J Craniomaxillofac Surg.* 2017;45(10):1593-1599.
22. Beasley RA. Medical Robots: Current Systems and Research Directions. *Journal of Robotics.* 2012;Volume 2012, Article ID 401613, 14 pages.
23. Kim VB, Chapman WH, Albrecht RJ, et al. Early experience with telemanipulative robot-assisted laparoscopic cholecystectomy using da Vinci. *Surg Laparosc Endosc Percutan Tech.* 2002;12(1):33-40.
24. Ghang MH, Kim HM, You JY, et al. Three-dimensional mandibular change after sagittal split ramus osteotomy with a semirigid sliding plate system for fixation of a mandibular setback surgery. *Oral Surg Oral Med Oral Pathol Oral Radiol.*

2013;115(2):157-166.
25. Kim DS, Woo SY, Yang HJ, et al. An integrated orthognathic surgery system for virtual planning and image-guided transfer without intermediate splint. *J Craniomaxillofac Surg.* 2014;42(8):2010-2017.
26. Kim SH, Kim DS, Huh KH, et al. Direct and continuous localization of anatomical landmarks for image-guided orthognathic surgery. *Oral Surg Oral Med Oral Pathol Oral Radiol.* 2013;116(4):402-410.
27. Han JJ. Development of splintless orthognathic surgery: Comparison of template-based orthognathic surgery and robot-arm and navigation assisted orthognathic surgery 2018.
28. Hirsch DL, Garfein ES, Christensen AM, Weimer KA, Saddeh PB, Levine JP. Use of computer-aided design and computer-aided manufacturing to produce orthognathically ideal surgical outcomes: a paradigm shift in head and neck reconstruction. *J Oral Maxillofac Surg.* 2009;67(10):2115-2122.
29. Coppen C, Weijs W, Berge SJ, Maal TJ. Oromandibular reconstruction using 3D planned triple template method. *J Oral Maxillofac Surg.* 2013;71(8):e243-247.
30. Hanasono MM, Skoracki RJ. Computer-assisted design and rapid prototype modeling in microvascular mandible reconstruction. *Laryngoscope.* 2013;123(3):597-604.
31. Uneri A, Balicki MA, Handa J, Gehlbach P, Taylor RH, Iordachita I. New Steady-Hand Eye Robot with Micro-Force Sensing for Vitreoretinal Surgery. *Proc IEEE RAS EMBS Int Conf Biomed Robot Biomechatron.* 2010;2010(26-29):814-819.
32. Hagn U, Konietschke R, Tobergte A, et al. DLR MiroSurge: a versatile system for research in endoscopic telesurgery. *Int J Comput Assist Radiol Surg.* 2010;5(2):183-193.
33. Wang X SR, Liu X, et al. System design for orthognathic aided robot. In: The 5th annual IEEE International Conference on cyber technology in automation, control and intelligent systems. 2015.
34. Burgner J TM, Vieira V, et al. System for robot assisted orthognathic surgery. *Int J Comput Assist Radiol Surg* 2007;2007:419-421.
35. Burgner J ZY, Raczkowsky J, et al. Methods for end-effector coupling in robot assisted invervention. *In: Robotics and automation, 2008 ICRA 2008 IEEE International Conference on Pasadena, CA, USA.* 2008.
36. Vieira VMM KG, Ionesco H, et al. Light-weight robot stability for orthognathic surgery. *Phantom and animal cadavar trials.* 2010;CURAC 2010:99-101.
37. Kang S-H. Maxillary Cutting Guide for Executing a Simulated Osteotomy and Removing the Bony Interference During Orthognathic Surgery. *Journal of Medical Devices.* 2015;Vol. 9.

TABLES

Table 1. Surgical movement for phantom experiments

Type of movement	Direction and amount of movement	Number of experiment
Bodily shift	Advancement (2 mm) + Total impaction(4 mm)	3
	Setback 3mm + Right 3mm	3
Rotation	Cant correction (#26 MBC: 3 mm up)	3
	Advance 3mm + Posterior impaction (#16: 4 mm upward)	3
Total		12

Abbreviations: #26 MBC, Mesiobuccal cusp of left maxillary second molar

Table 2. Mean absolute deviations of 8 reference landmarks on the osteotomy guide before and after fixation to the maxilla (mm)

Skull no.	M-D			A-P			S-I		
	Before fixation	After fixation	*p* value*	Before fixation	After fixation	*p* value*	Before fixation	After fixation	*p* value*
1	0.13 ±0.09	0.27 ±0.26	0.173	0.46 ±0.18	0.20 ±0.10	0.011	0.22 ±0.15	0.20 ±0.15	0.678
2	0.28 ±0.18	0.53 ±0.26	0.028	1.13 ±0.08	0.33 ±0.12	0.028	0.16 ±0.13	0.12 ±0.11	0.917
3	0.14 ±0.06	0.17 ±0.11	0.484	0.56 ±0.25	0.26 ±0.09	0.036	0.27 ±0.25	0.28 ±0.11	0.889
4	0.17 ±0.09	0.28 ±0.16	0.123	0.95 ±0.11	0.42 ±0.11	0.012	0.16 ±0.14	0.21 ±0.12	0.575
5	0.23 ±0.15	0.17 ±0.11	0.173	0.67 ±0.22	0.37 ±0.07	0.028	0.30 ±0.08	0.37 ±0.14	0.249
6	0.10 ±0.05	0.12 ±0.09	0.600	0.34 ±0.25	0.16 ±0.16	0.046	0.74 ±0.19	0.65 ±0.18	0.345
7	0.13 ±0.09	0.14 ±0.12	0.674	0.84 ±0.25	0.64 ±0.09	0.012	0.18 ±0.13	0.15 ±0.14	0.401
8	0.13 ±0.09	0.29 ±0.15	0.017	0.72 ±0.23	0.51 ±0.23	0.012	0.46 ±0.31	0.42 ±0.20	0.484
9	0.19 ±0.07	0.20 ±0.16	0.917	0.64 ±0.16	0.43 ±0.10	0.028	0.40 ±0.15	0.40 ±0.18	0.917
10	0.25 ±0.10	0.49 ±0.14	0.046	0.76 ±0.34	0.58 ±0.10	0.249	0.42 ±0.32	0.40 ±0.14	0.917
11	0.23 ±0.19	0.26 ±0.19	0.484	0.62 ±0.15	0.46 ±0.21	0.036	0.34 ±0.09	0.26 ±0.21	0.327
12	0.12 ±0.09	0.27 ±0.16	0.012	0.90 ±0.16	0.53 ±0.17	0.012	0.36 ±0.14	0.22 ±0.15	0.025
Total	0.17 ±0.12	0.26 ±0.20	0.000	0.71 ±0.28	0.41 ±0.20	0.000	0.32 ±0.23	0.30 ±0.20	0.233

Data are mean ± standard deviation

Abbreviations: M-D, medio-lateral direction; A-P, antero-posterior direction; S-I, supero-inferior direction

*By Wilcoxon signed-rank test for comparison between before- and after fixation in mean absolute deviations

Table 3. Root mean square deviation based on 8 reference landmarks before and after fixation to the maxilla (mm)

Skull no.	RMSD		
	Before fixation	After fixation	*p* value*
	Mean ± SD	Mean ± SD	
1	0.56 ± 0.16	0.44 ± 0.24	0.110
2	1.19 ± 0.09	0.68 ± 0.13	0.028
3	0.70 ± 0.15	0.43 ± 0.13	0.012
4	0.99 ± 0.10	0.59 ± 0.09	0.012
5	0.79 ± 0.22	0.57 ± 0.08	0.046
6	0.84 ± 0.25	0.70 ± 0.20	0.028
7	0.88 ± 0.25	0.69 ± 0.13	0.012
8	0.89 ± 0.32	0.76 ± 0.21	0.036
9	0.75 ± 0.21	0.65 ± 0.14	0.028
10	0.86 ± 0.31	0.87 ± 0.15	0.173
11	0.78 ± 0.13	0.66 ± 0.16	0.050
12	0.99 ± 0.17	0.68 ± 0.14	0.012
Mean	0.85 ± 0.24	0.64 ± 0.19	0.000

Abbreviations: RMSD, root mean square deviation; SD, standard deviation

*By Wilcoxon signed-rank test for comparison between before- and after fixation in mean absolute deviations

Table 4. Positioning accuracy of the osteotomy line using wall thickness analysis (mm).

Skull no.	Upper line Mean ± SD	Lower line Mean ± SD	All lines Mean ± SD
1	0.37 ± 0.37	0.83 ± 0.66	0.56 ± 0.56
2	0.38 ± 0.92	0.84 ± 0.61	0.48 ± 0.82
3	0.68 ± 0.51	0.39 ± 0.45	0.48 ± 0.49
4	0.20 ± 0.31	0.41 ± 0.49	0.27 ± 0.39
5	0.27 ± 0.43	0.57 ± 0.73	0.43 ± 0.63
6	1.00 ± 0.84	0.97 ± 0.81	0.99 ± 0.82
7	0.69 ± 0.51	0.41 ± 0.47	0.49 ± 0.50
8	0.22 ± 0.22	0.42 ± 0.49	0.28 ± 0.40
9	1.18 ± 0.79	0.39 ± 0.52	0.80 ± 0.78
10	0.32 ± 0.5	0.75 ± 0.53	0.45 ± 0.55
11	0.39 ± 0.52	0.22 ± 0.39	0.26 ± 0.44
12	0.15 ± 0.26	0.54 ± 0.51	0.24 ± 0.38
Total	0.49 ± 0.33	0.56 ± 0.23	0.48 ± 0.23
		p value 0.133	

Abbreviations: SD, standard deviation

*By Mann-Whitney U test for comparison of the accuracy between upper osteotomy line and lower osteotomy line

Table 5. Registration error of optical tracking system

Skull no.	Registration error
1	0.309
2	0.48
3	0.329
4	0.33
5	0.29
6	0.38
7	0.40
8	0.39
9	0.44
10	0.42
11	0.37
12	0.48
Total	0.38±0.06

Data are mean ± standard deviation

Table 6. Evaluation the accuracy of the head position returning process (mm)

Skull no.	M-D (m)	A-P (m)	*S-I* (m)	*RMSD*	Yaw(deg)	Pitch(deg)	*Roll*(deg)
1	0.99	0.7	1.08	1.62	0.056227	0.006467	0.057809
2	0.19	0.06	0.06	0.21	0.003406	0.000599	0.004548
3	0.02	0.09	0.02	0.09	0.000794	0.001307	0.000222
4	0.02	0.01	0.07	0.07	0.000616	0.000477	0.000682
5	0.06	0.02	0.11	0.13	0.003587	0.001218	0.005302
6	0	0.08	0.21	0.22	0.017907	0.003873	0.021453
7	0.13	0.04	0.44	0.46	0.04661	0.007449	0.050138
8	0.34	0.07	0.2	0.40	0.015548	0.002027	0.014203
9	0.3	0.02	0.09	0.31	0.001447	0.001922	0.004372
10	0.14	0.04	0.09	0.17	0.012437	0.000498	0.012169
11	0.02	0.03	0.03	0.05	0.006643	0.003146	0.007986
12	0.13	0.47	0.48	0.68	0.02162	0.001521	0.029439
Total	0.19 ± 0.27	0.14 ± 0.22	0.24 ± 0.30	0.37 ±0.44	0.01557 ± 0.182	0.00254 ± 0.002	0.01736 ± 0.019

Data are mean ± standard deviation

Abbreviations: M-D, medio-lateral direction; A-P, antero-posterior direction; S-I, supero-inferior direction

*

Table 7. Comparing accuracy of maxilla repositioning between manual mode by hands and using the smart pad (mm)

	M-D			A-P			S-I		
	Manual mode	Smart pad	*p* value*	Manual mode	Smart pad	*p* value*	Manual mode	Smart pad	*p* value*
	Mean + SD	Mean + SD	*p* value*	Mean + SD	Mean + SD	*p* value*	Mean + SD	Mean + SD	*p* value*
#11	0.74 ±0.27	0.37 ±0.26	0.008	0.65 ±0.49	0.29 ±0.29	0.010	0.55 ±0.28	0.39 ±0.43	0.136
#21	0.73 ±0.28	0.36 ±0.25	0.008	0.66 ±0.52	0.30 ±0.29	0.023	0.53 ±0.30	0.38 ±0.37	0.084
#13	0.66 ±0.26	0.31 ±0.19	0.004	0.73 ±0.48	0.32 ±0.22	0.025	0.65 ±0.30	0.28 ±0.19	0.004
#23	0.49 ±0.31	0.31 ±0.15	0.023	1.06 ±0.56	0.52 ±0.37	0.015	0.43 ±0.30	0.44 ±0.53	1.000
#16	0.37 ±0.33	0.30 ±0.25	0.638	0.81 ±0.64	0.52 ±0.47	0.307	0.69 ±0.41	0.44 ±0.24	0.117
#26	0.39 ±0.34	0.42 ±0.35	0.875	1.33 ±0.62	0.73 ±0.46	0.012	0.61 ±0.51	0.66 ±0.56	0.894
Pog	0.76 ±0.48	0.39 ±0.40	0.126	0.98 ±0.81	0.72 ±0.56	0.367	0.25 ±0.25	0.34± 0.32	0.209
Total	0.59 ±0.36	0.35 ±0.27	0.000	0.89 ±0.62	0.48 ±0.42	0.000	0.53 ±0.36	0.42 ±0.40	0.009

Data presented as mean ± standard deviation

Abbreviations: M-D, medio-lateral direction; A-P, antero-posterior direction; S-I, supero-inferior direction; SD, standard deviation

*By Wilcoxon signed-rank test for comparison between manual mode and using smart pad

Table 8. Differences in the root mean square deviation between manual mode and using smart pad (mm)

	RMSD		
	Manual mode	Smart pad	*p* value*
#11	1.23 ± 0.36	0.68 ± 0.48	0.002
#21	1.24 ± 0.36	0.67 ± 0.43	0.002
#13	1.25 ± 0.43	0.58 ± 0.23	0.002
#23	1.34 ± 0.48	0.88 ± 0.44	0.050
#16	1.25 ± 0.61	0.83 ± 0.44	0.071
#26	1.64 ± 0.57	1.28 ± 0.33	0.099
Pog	1.46 ± 0.60	0.97 ± 0.64	0.050
Total	1.34 ± 0.50	0.84 ± 0.48	0.000

Data presented as mean ± standard deviation

Abbreviations: RMS, root mean square deviation

*Based on Wilcoxon signed-rank test for comparison between manual mode and smart pad

Table 9. Mean absolute deviations based on the intraoperative navigation before and after fixation of the maxilla (mm)

	M-D			A-P			S-I		
	Before fixation	After fixation	*p* value*	Before fixation	After fixation	*p* value*	Before fixation	After fixation	*p* value*
#11	0.37 ±0.26	0.39 ±0.39	0.844	0.29 ±0.29	0.33 ±0.24	0.366	0.39 ±0.43	0.53 ±0.45	0.182
#21	0.36 ±0.25	0.33 ±0.40	0.689	0.30 ±0.29	0.37 ±0.31	0.272	0.38 ±0.37	0.53 ±0.44	0.157
#13	0.31 ±0.19	0.24 ±0.38	0.387	0.32 ±0.22	0.42 ±0.36	0.272	0.28 ±0.19	0.38 ±0.31	0.638
#23	0.31 ±0.15	0.29 ±0.36	0.783	0.52 ±0.37	0.61 ±0.46	0.637	0.44 ±0.53	0.64 ±0.46	0.065
#16	0.30 ±0.25	0.44 ±0.26	0.168	0.52 ±0.47	0.60 ±0.44	0.610	0.44 ±0.24	0.46 ±0.27	0.695
#26	0.42 ±0.35	0.56 ±0.35	0.209	0.73 ±0.46	0.76 ±0.42	0.398	0.66 ±0.56	0.63 ±0.49	0.754
Pog	0.39 ±0.40	0.55 ±0.40	0.325	0.72 ±0.56	0.90 ±0.74	0.286	0.34± 0.32	0.32 ±0.21	0.937
Total	0.35 ±0.27	0.40 ±0.37	0.329	0.48 ±0.42	0.57 ±0.47	0.045	0.42 ±0.40	0.50 ±0.39	0.044

Data presented as mean ± standard deviation

Abbreviations: M-D, medio-lateral direction; A-P, antero-posterior direction; S-I, supero-inferior direction

*By Wilcoxon signed-rank test for comparison between before- and after fixation in mean absolute deviations

Table 10. Root mean square deviation based on the intraoperative navigation before and after fixation of the maxilla (mm)

	RMSD		
	Before fixation	After fixation	*p* value*
#11	0.68 ± 0.48	0.85 ± 0.46	0.117
#21	0.67 ± 0.43	0.85 ± 0.47	0.050
#13	0.58 ± 0.23	0.75 ± 0.41	0.182
#23	0.88 ± 0.44	1.03 ± 0.59	0.224
#16	0.83 ± 0.44	0.98 ± 0.36	0.272
#26	1.28 ± 0.33	1.24 ± 0.51	0.610
Pog	0.97 ± 0.64	1.20 ± 0.71	0.108
Total	0.84 ± 0.48	0.99 ± 0.52	0.002

Data presented as mean ± standard deviation

Abbreviations: RMS, root mean square deviation

*By Wilcoxon signed-rank test

Table 11. Mean positional changes and root mean square deviation of the mobilized maxilla during fixation based on the intraoperative navigation (mm)

	M-D	A-P	S-I	RMSD
	Mean ± SD	Mean ± SD	Mean ± SD	Mean ± SD
#11	0.33 ± 0.15	0.23 ±0.15	0.40 ±0.31	0.62 ±0.25
#21	0.33 ± 0.15	0.23 ±0.15	0.40 ±0.30	0.62 ±0.24
#13	0.32 ± 0.16	0.24 ±0.18	0.39 ±0.30	0.63 ±0.24
#23	0.32 ± 0.18	0.16 ±0.06	0.47 ±0.37	0.65 ±0.31
#16	0.29 ± 0.22	0.35 ±0.34	0.42 ±0.16	0.70 ±0.27
#26	0.37 ± 0.33	0.32 ±0.44	0.59 ±0.43	0.85 ±0.58
Pog	0.30 ±0.26	0.38 ±0.22	0.29 ±0.28	0.66 ±0.24
Total	0.32 ±0.21	0.26 ±0.27	0.42 ± 0.32	0.68 ±0.32

Abbreviations: M-D, medio-lateral direction; A-P, antero-posterior direction; S-I, supero-inferior direction; RMSD, root mean square deviation; SD, standard deviation

Table 12. Mean absolute deviation between planned and actual postoperative maxillary position (mm)

	M-D	A-P	S-I
	Mean + SD	Mean + SD	Mean + SD
#11	0.57 ± 0.47	0.76 ± 0.49	0.41 ± 0.44
#21	0.50 ± 0.39	0.77 ± 0.41	0.43 ± 0.45
#13	0.47 ± 0.33	0.84 ± 0.58	0.38 ± 0.41
#23	0.46 ± 0.41	0.87 ± 0.43	0.49 ± 0.36
#16	0.32 ± 0.25	1.09 ± 0.70	0.44 ± 0.25
#26	0.35 ± 0.30	0.91 ± 0.33	0.63 ± 0.40
Total	0.45 ± 0.36	0.87 ± 0.50	0.46 ± 0.38

Abbreviations: M-D, medio-lateral direction; A-P, antero-posterior direction; S-I, supero-inferior direction; SD, standard deviation

Table 13. Root mean square deviation between planned and actual postoperative maxillary position (mm)

	RMSD
	Mean + SD
#11	1.22 ± 0.46
#21	1.15 ± 0.43
#13	1.18 ± 0.52
#23	1.21 ± 0.46
#16	1.27 ± 0.67
#26	1.26 ± 0.29
Total	1.22 ± 0.47

Abbreviations: RMSD, root mean square deviation; SD, standard deviation

Figure 1. Design of the maxillary osteotomy guide (A) Obtaining CBCT and preoperative virtual surgery using a 3D-simulation program. (B) Movement of the maxillomandibular complex to the planned position (C) Collision between two bony segments (blue) as the maxilla segment was repositioned. (D) Two osteotomy lines including interference area for removable during osteotomy. (E) Virtual guide template model with template cut by a pre-made virtual osteotomy line. (F) Placement of 8 landmarks and 8 cylinder-like models to prepare screw holes

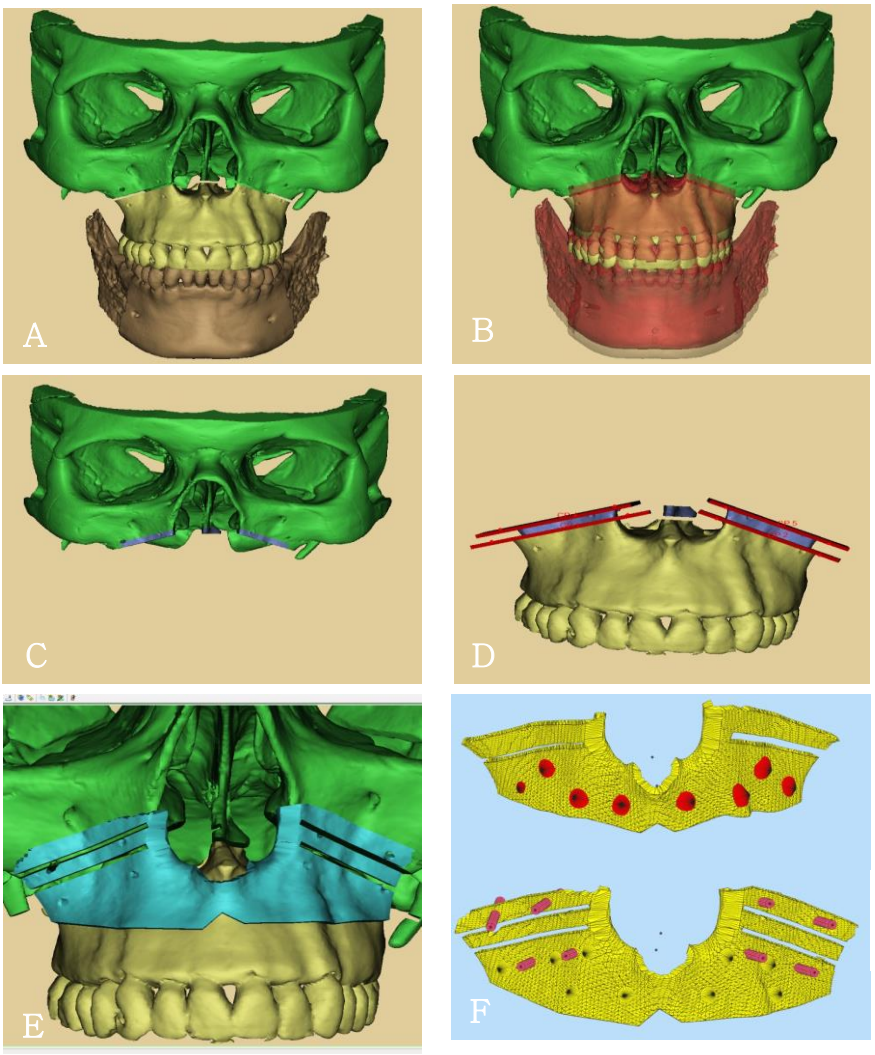

Figure 2. 3D-printed osteotomy guide placed and fixed with 8 mid screws on the anterior maxilla of a phantom skull

Figure 3. Evaluation of osteotomy guide positioning accuracy. (A) 3D CBCT of the maxilla at T0 with a virtual osteotomy guide. (B) Laser scan of an osteotomy guide with an osteotomized maxilla after surgery. (C) Superimpose laser-scanned image and pre-operative(T0) virtual image in a 3D CAD program. (D) Measured distances between landmarks.

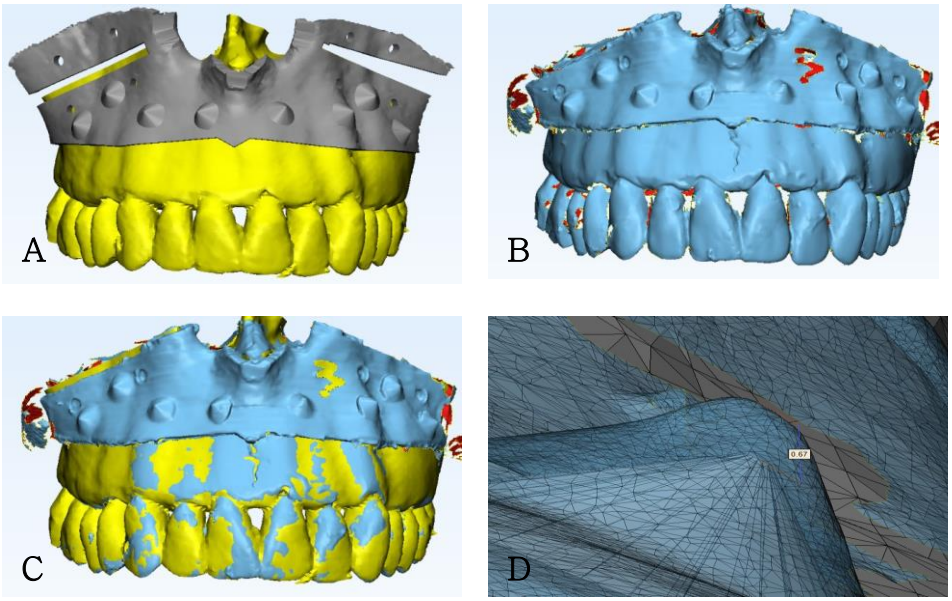

Figure 4. Accuracy of guided osteotomy line location. (A) Preoperative skull images with virtual osteotomy. (B) Postoperative skull images with actual osteotomy. (C) Planned and actual osteotomized maxilla upper and lower parts superimposed in a simulation program; overlapping parts were removed using boolean function. (D) Wall thickness analysis of the remaining portion of the maxillary front wall using the 3 matic CAD program (Materialise, Leuven, Belgium).

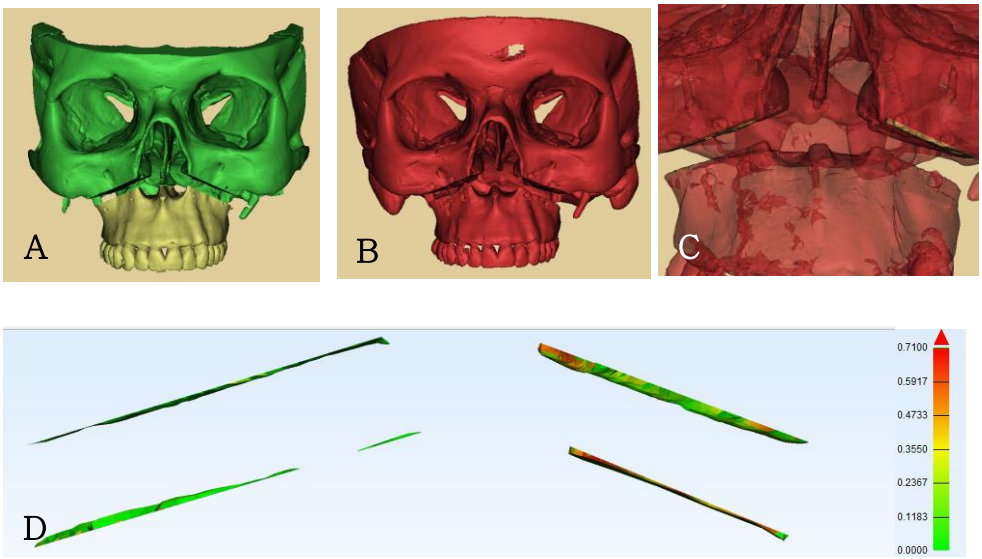

Figure 5. System for robot-arm and navigation system assisted orthognathic surgery.

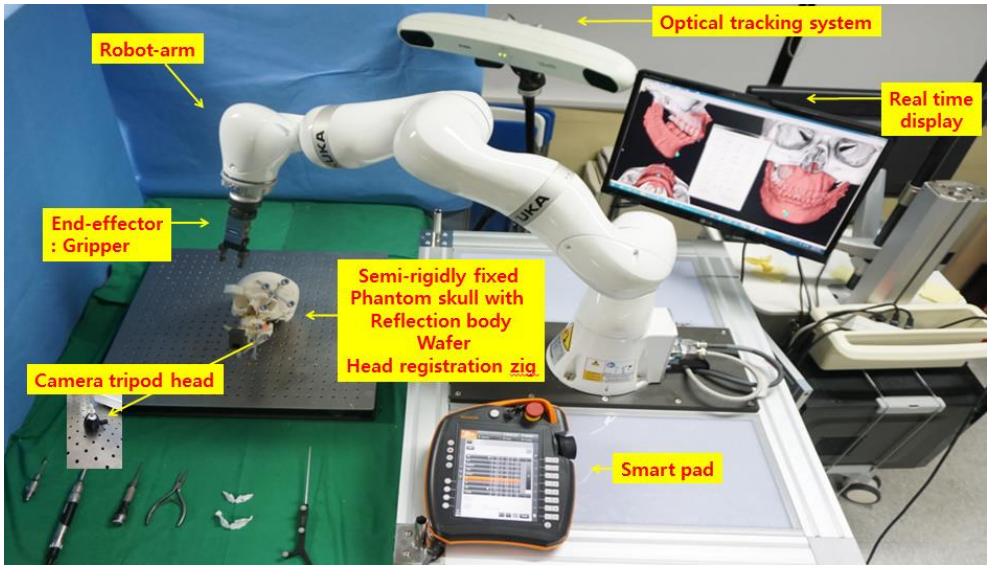

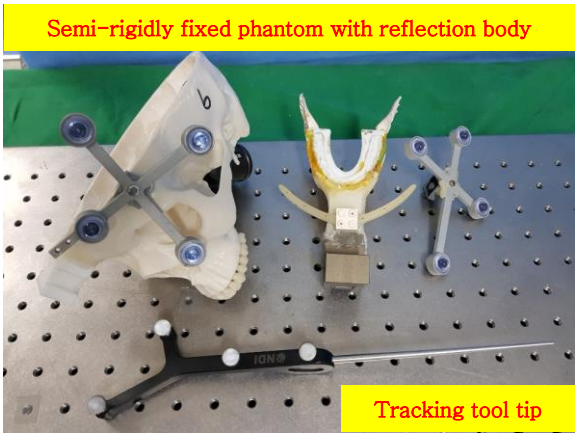

Figure 6. Development of CAD/CAM based connecting tools. (A) Virtual LeFort I osteotomy is performed on the 3D simulation program (B) The virtual horseshoe shape 3D mold is created about one-third the height of the tooth using program. Then, the virtual splint of the maxillomandibular dentition was designed using a subtraction function called Boolean. (C) Designed maxilla positioning splint was fabricated using 3D printer (D) Head registration zig was designed and fabricated using 3D printer and fixed on the supraorbital ridge. (E) MxP-splint connector that can be gripped by the end effector of the robot arm.

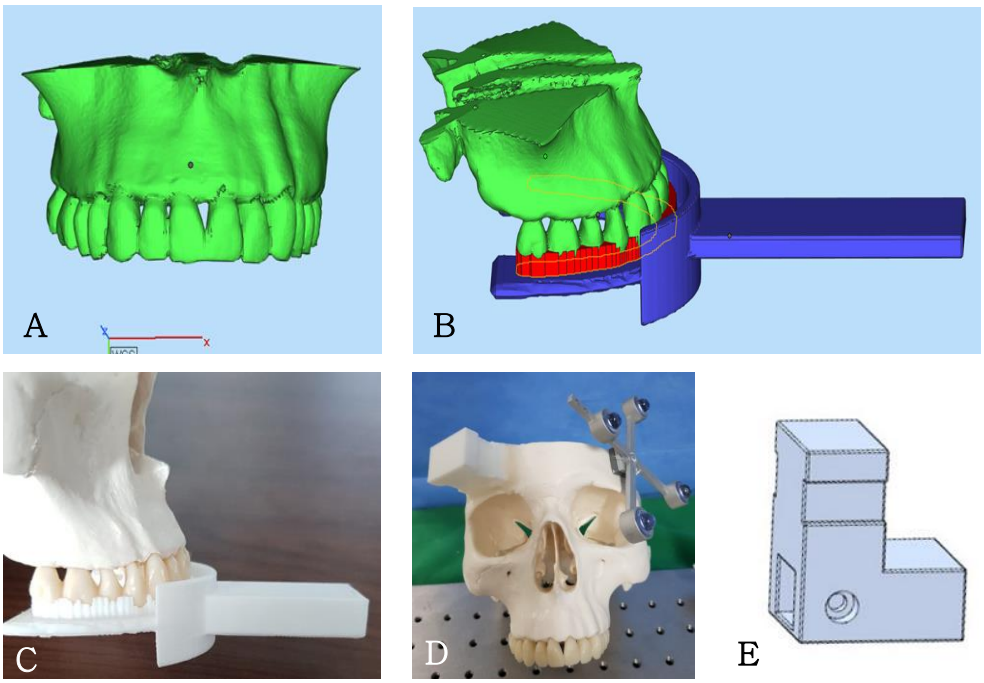

Figure 7. End-effector and phantom skull with connecting tools (MxP-splint, MxP-splint connector), optical tracking tools (Head, Maxillomandibular complex) and registration body.

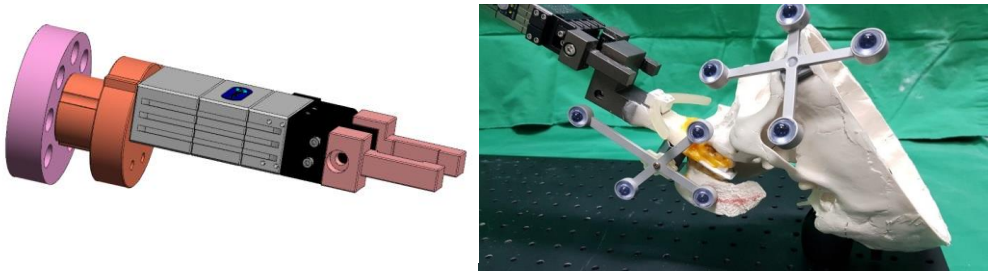

Figure 8. Flow chart of robot and navigation system assisted orthognathic surgery

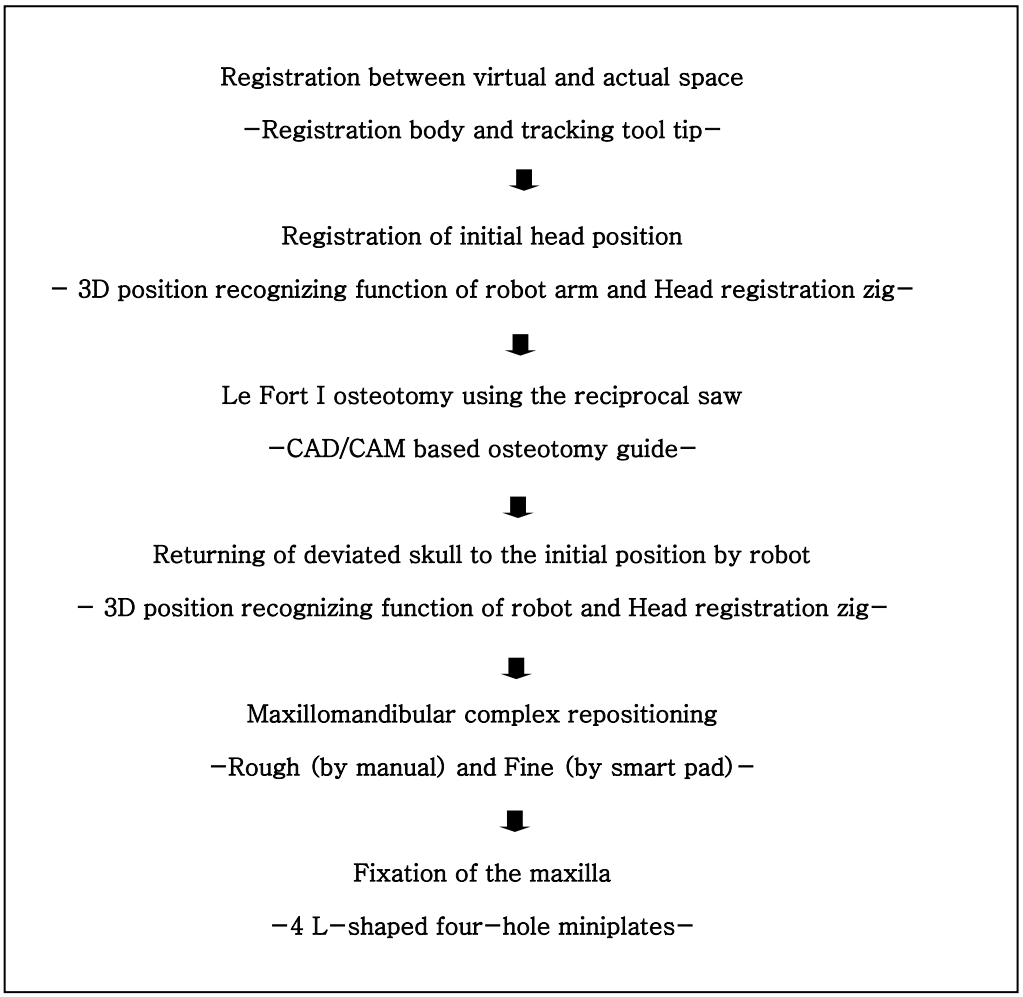

Figure 9. Registration process of the virtual space with actual space. (A) MxP splint with registration body was fixed to the maxillary teeth of the skull using sticky wax. (B) The CBCT(DENTRI-2; HDXWILL, Korea) images of (A) were acquired under 80 kVp and 10mA with a slice thickness of 0.20 mm. (C) Registration process of the actual space with virtual space using an optical tracking system and tracking tool tip

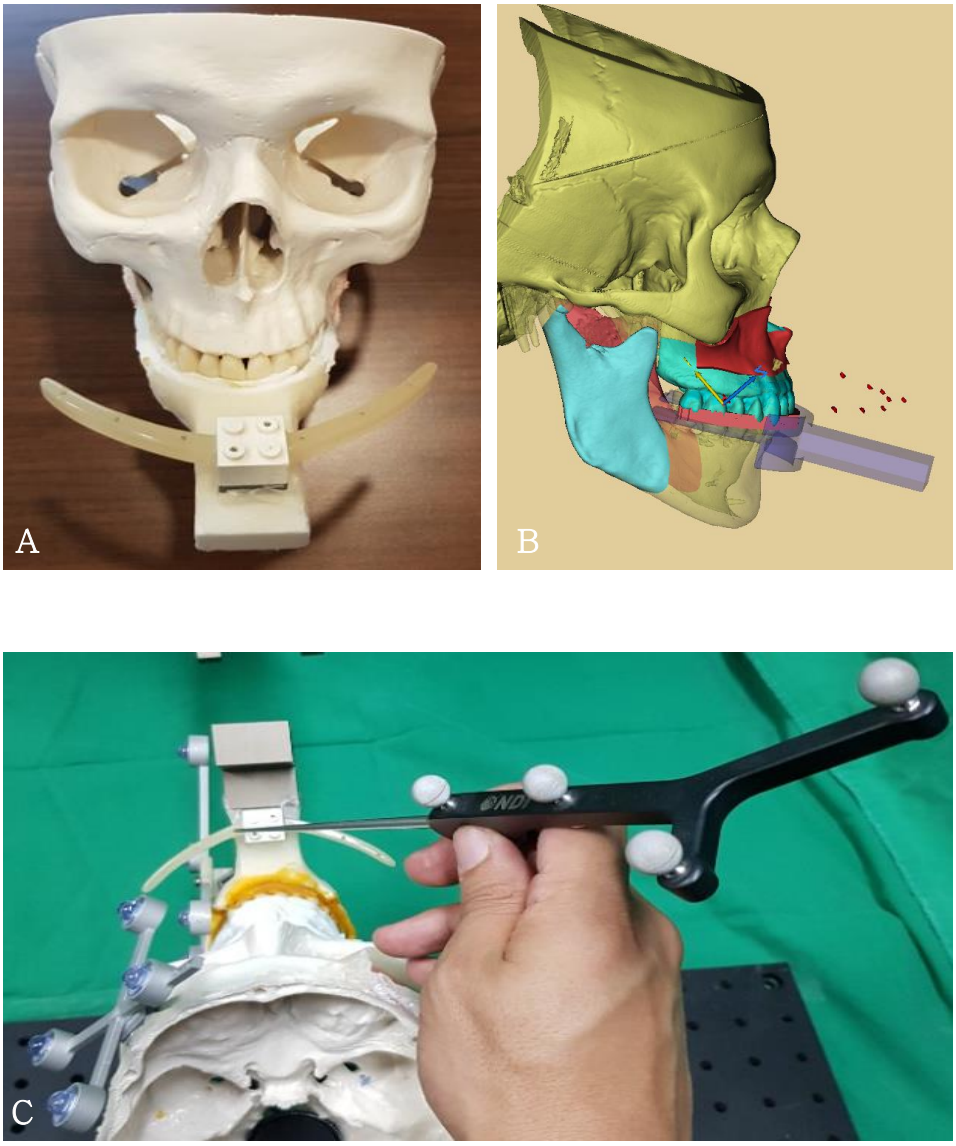

Figure 10. Registration of the initial head position using 3D position recognizing function of robot arm and head registration zig (H-zig).

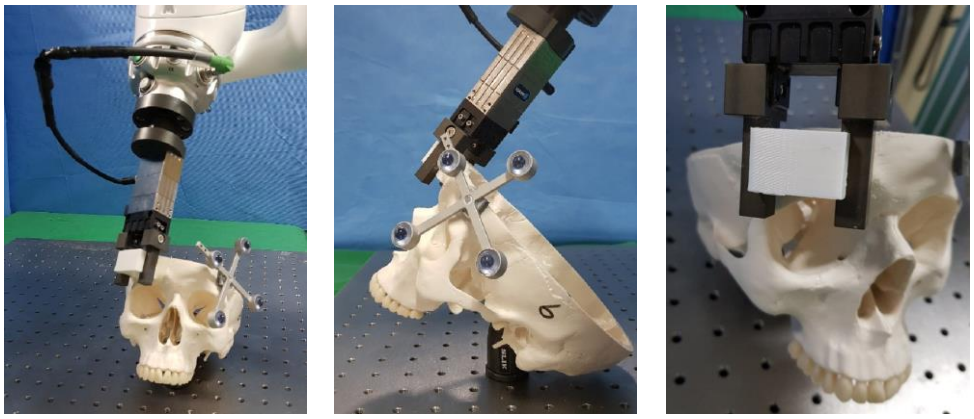

Figure 11. Maxillomandibular complex repositioning (A) While viewing the display screen, the robot arm manipulated by hand and moved as close as possible to the planned position. (B) Real-time display: tracking of the maxillomandibular segment using the intraoperative navigation system.

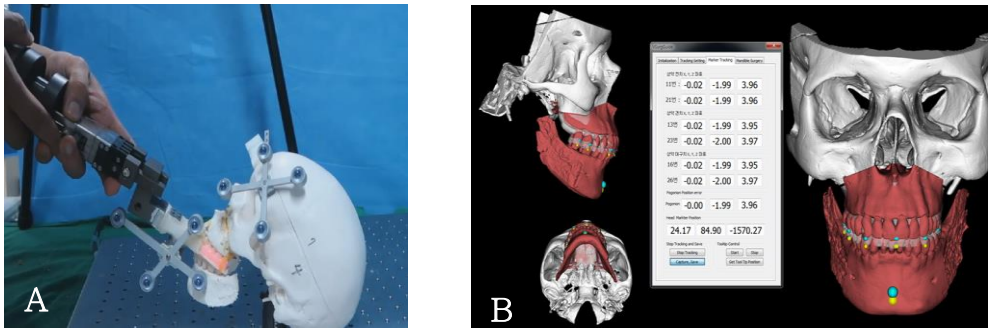

Figure 12. Fixation of the osteotomized maxillomandibular complex to the upper part using 4 L-shaped four-hole miniplates near the piriform aperture and zygomatic buttress area.

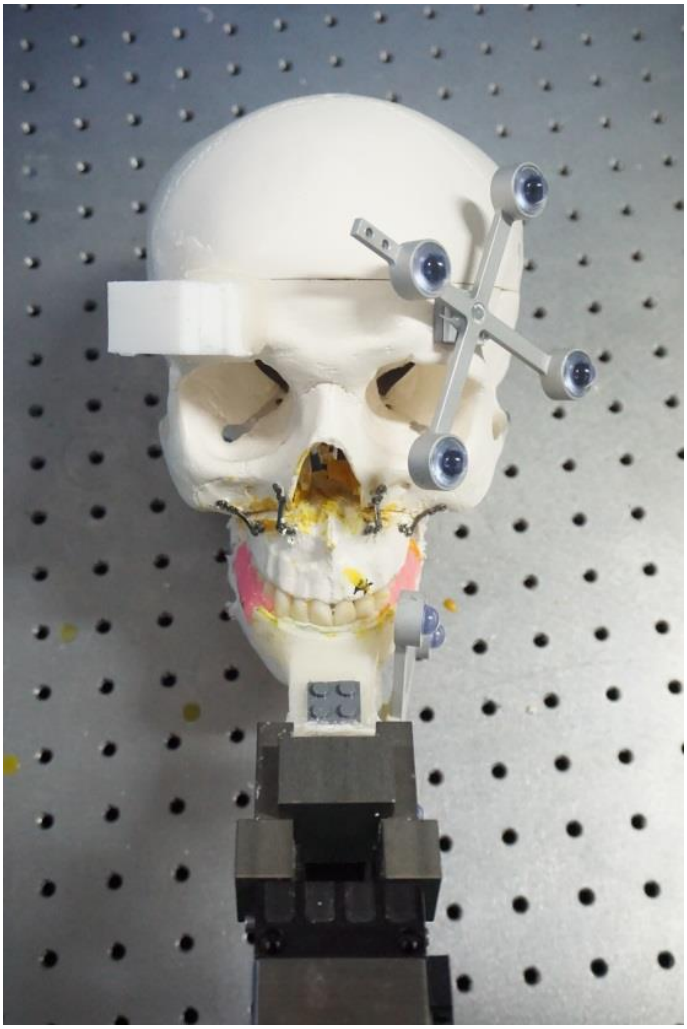

Figure 13. Comparison of planned location of maxilla from actual surgery using CBCT. (A) Since the CBCT data of the phantom skull are low in resolution, optical scan data of the cast model were obtained using a laser scanner. Laser scanned dentition is registered in the dentition of planned 3D skull model and dentition of the postoperative 3D skull model using point and global registration functions. (B) Both planned and postoperative 3D skull models merged with laser scanned dentition were imported into 3D CAD software (3-Matic, Materialise NV, Leuven, Belgium). Since the same scan data of the dental cast were used to register the pre-operative and post-operative 3D skull models, we can make a precise comparison by taking a point at the same position.

A

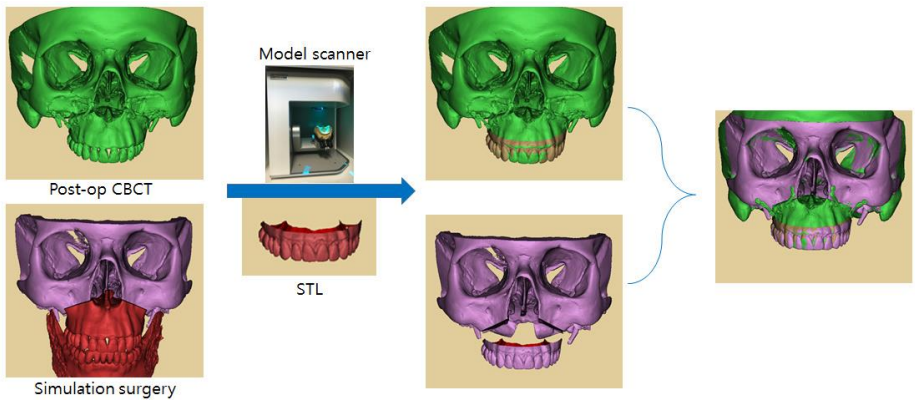

B

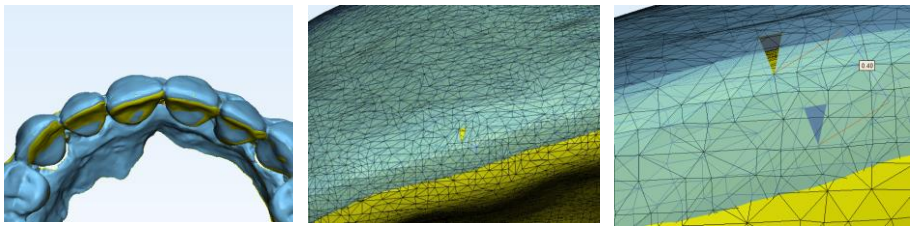

– 국문초록 –

턱교정수술에서 로봇의 3차원 위치 인식 기능과 네비게이션 시스템을 이용하여 두부 움직임의 조건에서 상하악 복합체 재위치 방법의 개발

박 재 봉

서울대학교 대학원 치의과학과 구강악안면외과학 전공

(지도교수 황 순 정)

연구 목적

본 연구에서는 7 자유도 (degree of freedom) 로봇의 3차원 위치 인식 기능과, 네비게이션 시스템을 사용하여 두부가 수술 중에 움직이는 조건 하에서 상하악 복합체를 수술 전 가상수술을 이용하여 결정한 계획대로 재위치 시키는 로봇 수술 방법을 개발하고 이에 대한 정확성을 평가 하고자 하였다.

또한, 르포트 1형 절골된 상악을 계획된 위치로 이동시킬 때 발생할 수 있는 충돌을 시뮬레이션 프로그램으로 미리 예측하여, 절골시 간섭 부분이 같이 삭제가 가능하도록 가이드를 제작하고, 그 정확성을 평가하였다.

연구 방법

총 12개의 skull 모형을 사용하였고, 4가지의 수술 계획에 따라

각각 3번의 실험을 반복하였다. 상하악 복합체의 재위치 및 절골가이드의 정확성을 평가하기 위해 3차원 CBCT, 레이저 스캐너, 네비게이션 시스템 그리고 3차원 CAD 프로그램을 사용하였다.

I. 절단된 상악골을 수술계획대로 재위치시킬 때 상악 기저골과 간섭되는 부분을 가상수술 프로그램을 통해 미리 확인하고, 골절단 과정에 간섭 부위를 같이 제거할 수 있도록, 3D 프로그램을 이용하여 골절단가이드를 디자인 후 3D 프린터로 출력하여 skull 모델에 적합시키고, 가이드를 나사로 고정하기 전과 후의 3차원 이미지를 레이저 스캐너로 채득하였다. 스캔한 상악 및 절골가이드 이미지와 수술 전 디자인한 가상의 절골 가이드 이미지를 3D 프로그램으로 중첩하여 가이드의 위치 정확성을 평가하였다.

상하악 복합체를 수술 계획에 따라 로봇으로 이동한 후 재위치 및 고정 하여 skull 모델의 CBCT를 촬영하고, 가상 수술을 진행한 3D skull 이미지와 중첩하여 골절단선의 정확성을 평가하였다.

II. 두부 움직임 조건에서, 7축 자유도 로봇의 3차원 위치 인식 기능과 내비게이션시스템을 이용하여 상악을 재위치 시키는 방법을 개발하였다.이를 위해 로봇팔과 두부 초기 위치 인식(registration) 지그(zig), 광학 추적 네비게이션 시스템이 사용되었으며, 두부와 상악골 상부자(splint)에 부착된 피추적 반사체(registration body)를 동시 추적하였다.

우선 두부 위치 인식 지그를 CAD/CAM 으로 제작하고 우측 상안와 부위에 고정한 뒤, 로봇 최종 작용체(end effector)를 결합하여 수술 전 두부의 위치를 기록하였다. 골절단가이드를 이용하여 르포트 1형 절골을 시행하고, 로봇에 저장된 위치정보와 머리 위치 인지 지그를 이용하여 두부를 수술 전 위치로 이동시켰다. 악골 수술 전 후 두부의 위치 차이를 네비게이션 시스템을 이용하여 확인하였고, 두부 재위치의 정확성을 평가하였다. 이후 로봇 팔을 상하악복합체 재위치용 스플린트와 연결하고, 실시간 네비게이션 영상을 보

면서 술자 손으로 로봇 팔을 움직여 계획된 위치에 최대한 가까이 이동시켰다. 이후 스마트 패드를 이용하여 로봇팔과 연결된 상악을 최종 위치로 밀리미터 이하 단위로 이동시켰다. 이동 중 충돌이 발생하면, 위치정보를 기록 후 분리시켜 간섭을 제거하고, 저장된 위치로 자동으로 되돌아가서 최종 위치를 맞추는 작업을 반복하였다. 시스템의 정확성을 평가하기위하여 술 중 내비게이션 및 술 후 전산화 단층 촬영 영상을 이용하였고, 최종적으로 수술 계획과 실제 수술 결과를 비교 · 분석하였다.

연구 결과

I. 3D 프린팅된 골절단 가이드의 상악골표면 적합 정확도는, 나사 고정 전, 계획된 위치와 비교하여 내외측으로 0.17 ± 0.12 mm, 전후방으로 0.71 ± 0.28 mm, 상하방으로 0.32 ± 0.23 mm 의 위치 변위를 보였으며, 나사 고정 후 내외측으로 026 ± 0.20 mm, 전후방으로 0.41 ± 0.20 mm, 상하방으로 0.30 ± 0.20 mm 의 위치 변화를 보였다. RMSD는 고정 전에 0.85 ± 0.24 mm, 고정 후에 0.64 ± 0.19 mm 를 보였다.

실제 골절단된 상악골 골편과, 가상 수술 한 3D 모델을 비교하였을 때, 절골선 위치의 정확도는, 상방 골절단선에서 0.49 ± 0.33 mm , 하방 골절단선에서 0.56 ± 0.23 mm의 평균 위치차이를 보였으며, 전체 골절단선 에서는 평균 0.48 ± 0.23 mm 의 차이를 보였다.

II. 두부 움직임조건하에서, 7축 로봇의 3차원 위치 인식 기능과 내비게이션 위치 추적 시스템을 이용하여 상하악 복합체를 계획대로 재위치시키는 방법을 개발하였다. 로봇 팔과 두부 위치 인식 지그를 이용하여 수술 전 skull의 두부 위치를 로봇에 저장하고, 저장된 정보를 이용하여 수술 후 skull의 두부 위치를 자동으로 수술 전과 같

은 위치로 이동 시켰을때, 정확도는 내외측으로 019 ± 0.27 mm, 전후방으로 0.14 ± 0.22 mm, 상하방으로 0.24 ± 0.30 mm, yawing 0.016 ± 0.132 deg, pitching 0.0025 ± 0.002 deg, rolling 0.0174 ± 0.019 deg의 변위를 보였다. RMSD 는 0.37 ± 0.44 mm 의 차이를 보였다.

술 중 내비게이션을 이용한 상악 재위치 정확도 평가에서 로봇을 술자가 네비게이션을 보면서 직접 손으로 이동 시켰을때는, 재위치된 상악골골편은 계획된 위치와 비교하여 0.59 ± 0.36 mm의 내외측 변위, 0.89 ± 0.62 mm의 전후방 변위, 0.53 ± 0.36 mm의 상하방 변위를 보였다. 로봇을 스마트 패드를 이용하여 밀리미터 이하 단위로 미세 조정 하는 방법으로 재위치된 상악골은 계획된 위치와 비교하여 0.35 ± 0.27 mm의 내외측 변위, 0.48 ± 0.24 mm의 전후방 변위, 0.42 ± 0.40 mm의 상하방 변위를 보였으며, RMSD 는 손으로 직접 움직였을때는 1.34 ± 0.50 mm 스마트 패드를 사용하였을 때는 0.84 ± 0.48 mm의 변위를 보였다.

재위치된 상악골 골편을 고정할 때, 상악골은 내외측으로 0.32 ± 0.21 mm, 전후방으로 0.27 ± 0.26 mm, 상하방으로 0.42 ± 032 mm 의 위치 변위를 보였다.

술 후 정확도 평가는 수술 후 콘빔 전산화 단층 촬영을 하여 3차원 가상수술 모델과 비교를 통해 분석하였으며 상악골의 계획된 위치와 비교하여 내외측 변위 0.45 ± 0.36 mm, 전후방 변위 0.87 ± 0.50 mm, 상하방 변위 0.46 ± 0.38 mm가 발생하였다. RMSD 는 1.22 ±0.47 mm 의 차이를 보였다.

결론

본 연구를 통해 두부 움직임 조건 하에서도 7축 로봇 팔의 3차원 위치인식 기능과 네비게이션 시스템의 도움으로 절골된 상악을 계획대로 위치시킬 수 있었으며, 그 정확도 또한 임상적으로 이용할만

가치가 확인되었다. 또한 시뮬레이션 프로그램 상에서 충돌 부분을 예측하여 골절단 시 간섭부위를 한번에 제거할 수 있도록 디자인한 골절단 가이드를 3D 프린팅 기술로 제작하여 사용하였고, 높은 정확성을 확인할 수 있었다.

주요어 : 악교정 수술, 골절단 가이드, 로봇, 3D 프린팅, 3차원 위치 인식 기능, 내비게이션, 정확도
학 번 : 2013-31193